01 Jan 1993

Flexural behavior of web elements with openings

Roger A. LaBoube
Missouri University of Science and Technology, laboube@mst.edu

Wei-Wen Yu
Missouri University of Science and Technology, wwy4@mst.edu

Ming-Yang Shan

Fifth Progress Report

Flexural Behavior of Web Elements with Openings

M.Y. Shan
R.A. LaBoube
W.W. Yu

January 1, 1993

Department of Civil Engineering
University of Missouri-Rolla
Rolla, Missouri

Fifth Progress Report

FLEXURAL BEHAVIOR OF WEB ELEMENTS WITH OPENINGS

M.Y. Shan, R.A. LaBoube, and W.W. Yu
Department of Civil Engineering
University of Missouri-Rolla
January 1, 1993

INTRODUCTION

The purpose of this research project has been to investigate the flexural behavior of C-shaped members with and without web openings. Common industry standard C-sections have been studied as summarized in the First, Second, Third, and Fourth Progress Reports (Refs. 1-4) and in this progress report. To date two test sequences have been completed at UMR. Test sequence No. 1 investigated sections with web openings fabricated from relatively low yield strength material. Test sequence No. 2 examined sections both with and without web openings. Specimens in test sequence No. 2 had yield strengths higher than those used for sequence No. 1. Test sequence No. 3 conducted by Reinhold M. Schuster (Ref. 5) is also reported herein. This report summarizes the UMR test procedure, the results and the evaluation of the research to date.

TEST SPECIMENS

Five sizes of C-sections were tested at UMR: 2.5-in., 3.625-in., 6-in., 8-in. and 12-in. web depths. Various thicknesses of each C-section were also tested. The cross-sectional dimensions, thickness and size of web openings for each test specimen are recorded in Tables 1-1, 1-2 and 1-3. The material properties of the steel, for each test specimen, were established by standard tensile coupon tests. Tables 2-1, 2-2 and 2-3 list the tensile test data for thickness, yield point, ultimate tensile strength and percent elongation in 2-in. gage length.

For all test sequences, the web openings were located at 24 inches on center as illustrated in Fig. 1. Test sequence No. 1 had two different web openings 4 x 1.5 inch and 2 x 0.75 inch, test sequence No. 2 had 4 x 1.5 inch openings only and test sequence No. 3 contains 4.02 x 1.50, 4.53 x 2.48, 4.65 x 1.69 and 4.61 x 2.52 inch perforated webs. The dimensions for test sequence No. 3 are converted from metric dimensions.

TEST SETUP

A similar test setup was used for all three test sequences, the following details pertain specifically to the UMR test setup.

Each test specimen consisted of two C-shaped beams connected together using 3/4 x 3/4 x 1/8 inch angles and self-drilling screws. See Fig. 2.

Each specimen was tested as a simply supported beam. Two concentrated loads were applied six feet apart positioning a hole at mid-span as shown in Fig. 1. This loading configuration provided a pure moment region between applied loads. The load was applied using a hydraulic jack. An electronic load cell placed between the jack and the cross beam measured the applied load. Figure 3 shows the test setup. For each test specimen, the span length and the "x" dimension are given in Tables 3-1, 3-2 and 3-3.

The ends of the beam were supported with vertical rollers to prevent lateral movement of the ends. See Fig. 4. In order to prevent premature failure of the beam due to lateral-torsional buckling, lateral bracing was also provided along the length of the span. A typical bracing scheme is shown in Figs. 4 and 5.

TEST PROCEDURE

For the UMR test program, each test specimen was loaded to failure. The load was applied to the test specimen in predetermined increments using a hydraulic jack. At each load increment the load and strain gauge readings were recorded to a data file. In addition, for each load increment the vertical displacement at midspan of the beam was measured by using a dial gauge. The load was increased in increments until the beam reached failure and could no longer sustain additional load.

TEST RESULTS

The applied failure load, P, for each test specimen is recorded in Tables 3-1, 3-2 and 3-3. The value of P is the load applied by the hydraulic jack at mid-span. Tables 4-1, 4-2 and 4-3 list the tested moment capacity, M_{ut}, for each specimen as well as the predicted moment capacity, M_{uc}, calculated according to the 1986 AISI Specification with the 1989 Addendum (Ref. 14). The dead load due to the cross beam and the test specimen have been accounted for in the moment calculations.

DISCUSSION OF TEST RESULTS

The moment ratio M_{ut}/M_{uc} is a measure of how well the AISI Specification estimates the bending strength of C-sections. Tables 4-1, 4-2 and 4-3 list the values of M_{ut}/M_{uc}. A discussion of the test results for each test sequence follows.

Test Sequence 1:

A total of 15 tests were conducted in this test sequence. The cross-sectional dimensions, material properties and test results are summerized in Tables 1-1, 2-1 and 3-1, respectively. Table 4-1 compares the tested and calculated moment capacities.

The ratio of M_{ut}/M_{uc} for the 2.5-in. deep sections varied from 0.947 to 1.046 and had a mean of 0.995. This moment ratio indicates good correlation between the tested and computed moments capacity. The 2.5-in. sections have an a/h ratio of 0.36.

For the 3.625-in. deep sections, the value of M_{ut}/M_{uc} ranged from 0.864 to 0.920 with a mean of 0.888. The lower ratios for the 3.625-in. sections are attributed to the presence of a punchout. For each test specimen, the failure occurred at the location of a punchout (Fig. 6). The punchout depth to web depth ratio, a/h, for these sections is 0.47.

For the 12-in. deep sections, the mean moment ratio, M_{ut}/M_{uc}, is 0.743 (Table 4-1). Based on the test results from test sequence No. 2 (Table 4-2), this low mean value is not being attributed to the presence of punchouts, but is believed to be caused by the flange-web interaction, commonly called distortional buckling. The narrow flange, nominally 1.625-in., does not appear to provide adequate edge restraint for the rather deep 12-in. web.

<u>Test Sequence 2</u>:

A total of 36 tests were conducted in test sequence No.2. The cross-sectional dimensions, material properties and test results for this sequence are summerized in Tables 1-2, 2-2 and 3-2, respectively. Table 4-2 compares the tested and calculated moment capacities.

The ratio of M_{ut}/M_{uc} for the 2.5-in. deep sections having web openings varied from 0.852 to 0.976 and had a mean of 0.924. For those without web openings the mean value of M_{ut}/M_{uc} was 1.086. The 2.5-in. deep sections have an a/h ratio of 0.74.

For the 3.625-in. deep sections the value of M_{ut}/M_{uc} ranged from 0.827 to 0.980 with a mean of 0.931 for test specimen with web openings. For test specimen without web openings the mean moment ratio was 1.096. The web punchout depth to web depth ratio, a/h, for these sections is 0.47.

The value of M_{ut}/M_{uc} varied from 0.647 to 1.002 and 0.774 to 1.069 for the 6-in. and 8-in. deep sections, respectively. For the

6-in. web, the narrow flange test specimens 6A (nominally 1.5-in.) has low moment capacities ranged from 0.793 to 0.818; whereas for 6B and 6C having wider flanges (nominally 2.0-in. and 2.5-in.), the tested and computed moments show a good moment ratio between 0.971 and 1.002. From Table 4-2, the 8-in. deep webs have the same behaviour as 6-in. web.

As indicated by Table 4-2, for the 12-in. deep sections, there was no significant difference in the tested moment capacity between C-sections with and without web openings. The ratio of M_{ut}/M_{uc} ranged from 0.755 to 0.788 with a mean of 0.772 for unpunched webs and ranged from 0.780 to 0.820 with a mean of 0.794 for punched webs.

As in test sequence No. 1, the narrow flange of the 6-in., 8-in. and 12-in. deep sections, may be experiencing distortional buckling. This may be the cause of the poor correlation between tested and calculated moment capacities.

Test Sequence 3:

A total of 17 tests were completed in test sequence No. 3 (Ref. 5). Tables 1-3, 2-3 and 3-3 present the cross-sectional dimensions, material properties and test results, and Table 4-3 presents the comparison of the tested and calculated moment capacities.

For the 8-in. deep sections (Table 4-3), the ratio of M_{ut}/M_{uc} ranged from 0.756 to 0.839 with a mean 0.790 for solid web specimens and ranged from 0.750 to 0.857 with a mean 0.816 for perforated web elements. This poor performance may be attributed to distortional buckling.

Based on the results of these three studies, (test sequences 1, 2 and 3), the 6-in., 8-in. and 12-in. deep channel sections having small lip stiffeners, and narrow flanges yielded poor predicted moment capacities. The local buckling mode was not present for these sections. These specimens failed in a distortional buckling mode. The failure did not necessarily occur at the location of holes, whereas, the specimens with shallower webs failed by local buckling near a punchout. Fig. 6 shows typical local buckling failures. Postbuckling strength was present for both local and distortional buckling failure modes.

MOMENT CAPACITY CALCULATION

For test specimens that failed by local buckling and yielding, the test data (Tables 4-1 and 4-2) indicates that for certain geometries, the moment capacity predicted by the AISI Specification can not be achieved. Therefore, three alternate ways to compute the moment capacity have been examined.

Method I : AISI Formula Using Modified Effective Web Area

Tables 5-1 and 5-2 show the results of an analysis of the moment capacity in which the value of b_2 as given in section B2.3 of the AISI Specification was set equal to zero (Fig. 7). The combined data from test sequences No. 1 and 2 will be discussed.

For test specimens having a/h ratios of approximately 0.36, it appears no modification is necessary (Table 4-1). The mean moment ratio for test sequence No. 1 is 0.995.

For test specimens having an a/h ratio of about 0.47, the mean moment ratio without the $b_2=0$ modification is 0.909 and with the modification is 0.956.

For test specimens with an a/h ratio of approximately 0.74, the mean moment ratio is 0.924 without the $b_2=0$ modification, and 0.974 when b_2 equals zero.

The $b_2=0$ modification was not applied to the 12" deep sections because the premature failure of these sections does not appear to be caused by local buckling resulting from the presence of a web punchout.

Method II : Net Section Approach

Employing the net section (Fig. 8) to compute the ultimate bending moment, M_{ufn}, results in moment capacities as summarized in Tables 6-1 and 6-2.

For test specimens having an a/h ratio of approximately 0.36, the mean moment ratio was 1.021 when the section modulus was computed using the net section.

For both test sequences with a/h ratio of about 0.47, the mean moment ratio M_{ut}/M_{ufn} is 0.939.

For test specimens having an a/h ratio of around 0.74, the mean moment ratio is 1.093 using the net section.

Method III : Effective Net Section Approach

The net section moment capacity (Method II), M_{ufn}, does not recognize the potential for a reduction in moment capacity that may occur due to local buckling of the web and flange. To account for postbuckling strength, the effective width concept was used. The local buckling in the flange was accounted for by using the current AISI effective width equations for edge stiffened compression elements. To reflect the influence of web local buckling, the portion of the web above the web punchout was treated as an unstiffened compression element with the buckling coefficient taken as 0.43 (Fig. 9). For each test specimen, the computed moment capacity, M_{uen}, is given in Tables 7-1 and 7-2.

For test specimens having a/h of approximately 0.36, the mean moment ratio, M_{ut}/M_{uen} is 1.031.

For both test sequences with a/h ratio of about 0.47, the mean value for the ratio of M_{ut}/M_{uen} is 0.984.

For test specimens having an a/h ratio of around 0.74, the mean moment ratio is 1.096.

Based on the above analysis of three different methods, Table 8 summaries the results of the comparison of the tested to computed moment capacities.

DISTORTIONAL BUCKLING BEHAVIOR

As previously discussed, the results in Tables 4-1, 4-2 and 4-3 based on the local buckling failure of the web did not account for the distortional buckling effects. Channel sections and other sections of monosymmetry may undergo a mode of buckling called distortional buckling, in which the lip-stiffened flange of the section rotates about the flange-web junction. A detailed study on the distortional mode was presented by Hancock in 1985 (Ref 6).

Distortional buckling will usually occur in the flanges of channel sections if the lip stiffener is inadequate to prevent its moment normal to the plane of the flange, so the distortional mode of buckling may control the design for some specimens, especially sections with small lip stiffeners or flanges.

The difference between local and distortional buckling mode is shown in Fig. 10. Because the slender web is unreinforced and the lip stiffeners and flanges are small, the distortional buckling mode will exist even though there are angles connecting the test specimens on the top and bottom in the test setup.

ANALYTICAL FORMULATIONS

The following discussion is based on two approximate models for considering the distortional buckling.

Model A:

The approximate theoretical model shown in Fig. 11 was derived by Sammy C.W. Lau and Gregory J. Hancock in 1987 (Ref. 7). The effects of the web on the flanges are represented by a lateral spring and a rotational spring. By considering equilibrium of forces in the plane of x and y directions and the equilibrium of moments about the shear center, three simultaneous differential equations were determined as follows:

$$EI_y\frac{d^4u}{dz^4}+EI_{xy}\frac{d^4v}{dz^4}+P(\frac{d^2u}{dz^2}-y_o\frac{d^2\phi}{dz^2})+k_x[u+(y_o-h_y)\phi]=0 \qquad \text{(Eq. 1)}$$

$$EI_x\frac{d^4v}{dz^4}+EI_{xy}\frac{d^4u}{dz^4}+P(\frac{d^2v}{dz^2}-x_o\frac{d^2\phi}{dz^2})+Q_y=0 \qquad \text{(Eq. 2)}$$

$$EI_w\frac{d^4\phi}{dz^4}-(GJ-\frac{I_o}{A}P)\frac{d^2\phi}{dz^2}-P(x_o\frac{d^2v}{dz^2}-y_o\frac{d^2u}{dz^2})$$
$$+k_x[u+(y_o-h_y)\phi](y_o-h_y)-Q_y(x_o-h_x)+k_\phi\phi=0 \qquad \text{(Eq. 3)}$$

where u,v, and ϕ are the horizontal, vertical, and rotational displacements, and k_x and k_ϕ are the horizontal and rotational restraints.

The general solutions were obtained by solving simultaneous differential equations 1 to 3.

By applying several simplifications, the design formula for the distortional buckling load as given by Lau and Hancock, P_{cr}, can be expressed as follows (Ref. 7):

$$P_{cr}=\frac{E}{2}[(\alpha_1+\alpha_2)+\sqrt{[(\alpha_1+\alpha_2)^2-4\alpha_3]}] \qquad \text{(Eq. 4a)}$$

$$\text{where } \alpha_1=\frac{\eta}{\beta_1}(I_xb_f^2+0.039J\lambda^2)+\frac{k_\phi}{\beta_1\eta E} \qquad \text{(Eq. 4b)}$$

$$\alpha_2=\eta(I_y+\frac{2}{\beta_1}\bar{y}b_fI_{xy}) \qquad \text{(Eq. 4c)}$$

$$\alpha_3=\eta(\alpha_1I_y-\frac{\eta}{\beta_1}I_{xy}^2b_f^2) \qquad \text{(Eq. 4d)}$$

$$\beta_1=\overline{x}^2+\frac{(I_x+I_y)}{A} \quad \text{(Eq. 4e)}$$

$$\beta_2=I_w+I_x(x_o-h_x)^2 \quad \text{(Eq. 4f)}$$

$$\beta_3=I_{xy}(x_o-h_x) \quad \text{(Eq. 4g)}$$

$$\beta_4=\beta_2+(y_o-h_y)\,[I_y(y_o-h_y)-2\beta_3] \quad \text{(Eq. 4h)}$$

$$\lambda=4.80\left(\frac{I_x b_f^2 b_w}{t^3}\right)^{0.25} \quad \text{(Eq. 4i)}$$

$$\eta=\left(\frac{\pi}{\lambda}\right)^2 \quad \text{(Eq. 4j)}$$

The distortional buckling stress, σ_d, is obtained as

$$\sigma_d=\frac{P_{cr}}{A} \quad \text{(Eq. 5)}$$

where A is the gross section area of the flange and edge stiffener as defined and shown in Fig. 11.

The nominal elastic or inelastic distortional buckling stress, F_d, is given by (Ref. 12):

$$F_d=F_y\left(1-\frac{F_y}{4\sigma_d}\right) \quad ; \text{ when } \sigma_d \geq \frac{F_y}{2} \quad \text{(Eq. 6a)}$$

$$F_d=F_y\left[0.55\left(\sqrt{\frac{F_y}{\sigma_d}}-3.6\right)^2+0.237\right] \quad ; \text{ when } \sigma_d < \frac{F_y}{2} \quad \text{(Eq. 6b)}$$

and the nominal moment is obtained as:

$$M_{uc,d} = F_d \, S_{ex} \qquad \text{(Eq. 7)}$$

where S_{ex} is the effective section modulus without consideration of web openings.

The rotational restraint, k_ϕ, as derived by Lundquist, Stowell, and Schuette (Ref. 8), and rederived by Lau and Hancock (Ref. 9) approaches a constant of $2D/b_w$ (Eq. 8b).

$$k_\phi = \frac{Et^3}{5.46\,(b_w + 0.06\lambda)} \qquad \text{(Eq. 8a)}$$

$$k_\phi = \frac{2D}{b_w} = \frac{Et^3}{5.46 b_w} \qquad \text{(Eq. 8b)}$$

$$k_\phi = \frac{Et^3}{4.00 b_w} \qquad \text{(Eq. 8c)}$$

Equation 8b was subsequently adjusted by Lau and Hancock to provide correlation with a finite strip analysis, and is given by Eq. 8a. Equation 8c was employed by Charnvarnichborikarn (Ref. 10) when investigating the distortional buckling mode of Z-sections.

Based on the approximate theoretical mode A, four possible methods have been investigated for the strength of beam members.

(i) Method I: $M_{uc,d} = F_d \, S_{ex,Fy}$

Using the different k_ϕ values of the above Eqs. 8a to 8c, and the effective section modulus calculated by using the yielding stress when evaluating the equations of effective width in AISI Specification (Fig. 12a), $M_{uc,d}$ was computed and is shown in Tables 9-1, 9-2 and 9-3 for the three test sequences.

(ii) Method II: $M_{uc,d} = F_d \, S_{ex,d}$

Another approach for computing $M_{uc,d}$ is to use the effective width of web, flange and lip stiffener (Fig. 12b) which accounts for the distortional buckling behaviour and F_d (Eqs. 6a and 6b) to calculate the ultimate moment. The effective width formulas for the distortional buckling as given by Lau and Hancock (Ref. 11) were used and are as follows:

$$\frac{b_e}{b}=1 \quad ; \quad \lambda \le 0.561 \qquad \text{(Eq. 9a)}$$

or

$$\frac{b_e}{b}=\left(\frac{\sigma_d}{F_y}\right)^{0.6}\left[1-0.25\left(\frac{\sigma_d}{F_y}\right)^{0.6}\right] \quad ; \quad \lambda > 0.561 \qquad \text{(Eq. 9b)}$$

$$\text{where} \quad \lambda=\sqrt{\frac{F_y}{\sigma_d}} \qquad \text{(Eq. 9c)}$$

$$P_{cr}=\text{(Eq. 4a)}$$

The comparison of tested and computed moment is shown in Tables 10-1, 10-2 and 10-3 for three sequences.

(iii) Method III: $M_{uc,d}= F_d\ S_{ex,Fd}$

Another possible way to predict the moment capacity is shown in Tables 11-1, 11-2 and 11-3 which present the results by using the nominal elastic or inelastic distortional buckling stress (Eqs. 8a and 8b) substituted into the formulas of the AISI Specification for the web, and Eqs. 9a, 9b and 9c for the flange and edge stiffener which account for the distortional buckling mode. The effective section modulus, $S_{ex,Fd}$, was defined as shown by Fig. 12c.

(iv)Method IV: $M_{uc,d} = F_d \, S_{ex,dy}$

The effective section modulus, $S_{ex,dy}$, shown in Fig. 12d was determined by using the elastic or inelastic distortional buckling stress, F_d, substituted into the equations of effective width in AISI Specification. The computed moment, $M_{uc,d}$, was obtained to compare the test moment. The results of M_{ut}, $M_{uc,d}$ and the ratio of $M_{ut}/M_{uc,d}$ are shown in Tables 12-1, 12-2 and 12-3 for three sequences.

Model B:

Using the model shown in Fig. 13, another moment expression for distortional buckling stress with constraints defined by rotational and extensional springs located at the web-tension flange junction was evaluated. This model, which assumes that distortional buckling occurs before local buckling, was developed by Serrette and Pekoz (Refs. 12 and 13). In this model, no lateral displacement is allowed at the web-tension flange junction because the whole section is assumed to be laterally stable. Also, two differential equations for flexure about x and y axes respectively, and one equation for the equilibrium of moments about the shear center were developed. The solutions for the elastic distortional buckling moment, $M_{cr,d}$, is given as:

$$M_{cr,d} = \frac{\alpha_1 + \alpha_2}{\alpha_3} \qquad \text{(Eq. 10a)}$$

$$\text{where} \quad \alpha_1 = (EI_{xy}\eta\theta^2 + k_y\xi)^2 \qquad \text{(Eq. 10b)}$$

$$\alpha_2 = -(EI_x\theta^2 + k_y)(EC_w\theta^2 + EI_y\eta^2\theta^2 + GJ\theta + k_y\xi^2 + k_\phi) \qquad \text{(Eq. 10c)}$$

$$\alpha_3 = -(2\eta + \beta_1)(EI_x\theta^2 + k_y)\theta \qquad \text{(Eq. 10d)}$$

$$\eta = y_o - h_y \qquad \text{(Eq. 10e)}$$

$$\xi = x_o - h_x \qquad \text{(Eq. 10f)}$$

$$\theta = \frac{\pi^2}{L_e^2} \qquad \text{(Eq. 10g)}$$

$$L_e = k_1 L_u \qquad \text{(Eq. 10h)}$$

$$k_\phi = \frac{Et^3}{(1-\nu^2)(6w_f + 4w_w)}\gamma \qquad \text{(Eq. 10i)}$$

The elastic buckling stress, $F_{cr,d}$, is expressed as:

$$F_{cr,d} = \frac{M_{cr,d}}{S_g} \qquad \text{(Eq. 11)}$$

where S_g is the gross section modulus for the section shown by Fig. 13b, and the nominal compressive stress, F_n, is determined as follows:

$$F_n = F_{cr,d} \quad ; \quad F_{cr,d} \le \frac{F_y}{2} \qquad \text{(Eq. 12a)}$$

$$F_n = F_y \left(1 - \frac{F_y}{4F_{cr,d}}\right) \quad ; \quad F_{cr,d} > \frac{F_y}{2} \qquad \text{(Eq. 12b)}$$

where F_y is the yield strength of the material

Finally the ultimate moment, $M_{uc,d}$, is computed by:

$$M_{uc,d} = F_n \, S_e \qquad \text{(Eq. 13)}$$

where S_e is the effective section modulus determined by using the AISI (1986) effective width provisions.

(v)Method V: $M_{uc,d} = F_n \, S_e$

Based on the above design procedure (Eq. 13), the tested moment, M_{ut}, computed moment, $M_{uc,d}$, and the ratio of $M_{ut}/M_{uc,d}$ are presented in Tables 13-1, 13-2 and 13-3 for three sequences.

DISCUSSION OF THE TEST RESULTS FOR DISTORTIONAL BUCKLING MODE

Based on the discussion in the previous section (models A and B), five possible methods have been investigated to design the beam members subjected to distortional buckling. The computed ultimate bending moments corresponding to each method have been evaluated and are discussed in the following:

(i)Method I: $M_{uc,d} = F_d \, S_{ex,Fy}$

An analysis of $M_{uc,d}$ based on the effective section modulus calculated by using the yielding stress and equations of effective width in AISI Specification and F_d with k_ϕ defined by Eq. 8c is summarized in Table 9-4 and has a mean moment ratio of 1.014 for the combination of all three test sequences. This leads to a slightly better comparison than by using the other k_ϕ values (Eqs. 8a and 8b). Using Eq. 8b for the computed moment, the mean ratio of $M_{ut}/M_{uc,d}$ is 1.119 for test sequence No. 2, 1.079 for test sequence No. 3 and 1.067 for combined three sequences shown in Table 9-4.

(ii)Method II: $M_{uc,d}= F_d\ S_{ex,d}$

For the $M_{uc,d}$ determined by using the effective section modulus based on Eqs. 9a, 9b and 9c and applying k_ϕ Eqs. 8a, 8b, and 8c, the mean moment ratios are summaried in Table 10-4. An examination of Table 10-4 indicates that the mean ratio of $M_{ut}/M_{uc,d}$ is 1.023 for test sequence No. 2, 1.110 for test sequence No. 3 and 1.046 for combined three sequences. Applying the theoretical values of rotational restraint, k_ϕ, in Eq. 8b and effective section modulus, $S_{ex,d}$, is a good method to predict the moment capacity.

(iii)Method III: $M_{uc,d}= F_d\ S_{ex,Fd}$

The computed moment, $M_{uc,d}$, was also computed using the AISI effective width equations with $f=F_d$ for the web, and using the formulas, Eqs. 6a and 6b, with $f=F_d$ for the flange, where F_d is computed for each of the possible k_ϕ equations (Eqs. 8a, 8b, and 8c). When using k_ϕ Eq. 8b, Table 11-4 demonstrates a mean moment ratio about 1.104 for test sequence No. 2 and 1.098 for three sequences.

(iv)Method IV: $M_{uc,d}= F_d\ S_{ex,dy}$

Applying the elastic or inelastic distortional buckling stress, F_d, and the equations of effective width in the AISI Specification to determine the effective section modulus, the computed moment, $M_{uc,d}$, was obtained. By using k_ϕ Eq. 8a, the ratios of $M_{ut}/M_{uc,d}$ in Table 12-4 have an average value of 1.009 for three sequences. Employing Eq. 8b for k_ϕ, Table 12-4 presents that the test sequence No. 1 has a mean moment ratio of 0.859 and test sequence No. 2 and No. 3 both have a mean moment ratio of 1.004. The ratio of $M_{ut}/M_{uc,d}$ ranged from 0.753 to 0.998 in test sequence No. 1 and results in the mean moment ratio of 0.988 for three sequences; this is an acceptable approach to compute the ultimate bending moment. Using Eq. 8c overestimates the moment capacity for three sequences.

(v) Method V: $M_{uc,d} = F_n S_e$

When appling mode B to determine the $M_{uc,d}$, all three sequences have a very conservative ratio of $M_{ut}/M_{uc,d}$ shown in Tables 13-1, 13-2 and 13-3.

BUCKLING COEFFICIENT

Because of the complicated calculations for distortional buckling behavior (Eqs. 4a to 4j), an investigation was undertaken to modify the effective width equations of the AISI Specification. The intent is to derive an appropriate web buckling coefficient that will reflect the distortional buckling behavior, rather than local buckling behavior.

From Section B2 of the AISI Specification, the buckling coefficient, k, is calculated as follow:

$$k=4+2(1-\psi)^3+2(1-\psi) \quad \text{(Eq. 14a)}$$

$$\psi=\frac{f_2}{f_1} \quad \text{(Eq. 14b)}$$

where f_2 and f_1 are calculated on the basis of effective section (Fig. 7). Equations 14a and 14b were developed to illustrate the local buckling behavior of the C-Channel sections, and do not reflect the distortional buckling behavior for the test specimens. Based on an analysis of the test data, the web buckling coefficient for distortional buckling varied from 1.00 to 9.80. This compares to a web local buckling coefficient of 20 to 24. Based on a regression analysis of the data shown by Figs. 14a and 14b, the buckling coefficient, k, may be represented by one of the following equations:

$$k=-897.78-3810.42\psi-5368.78\psi^2-2520.34\psi^3 \quad \text{(Eq. 15a)}$$

$$k=-1134.69+34215.84\left(\frac{w}{h}\right)-374719.92\left(\frac{w}{h}\right)^2+1762857.65\left(\frac{w}{h}\right)^3-3002545.11\left(\frac{w}{h}\right)^4 \quad \text{(Eq. 15b)}$$

$$k=70.34+240.94\psi+182.70\psi^2+162.94\left(\frac{w}{h}\right)-543.90\left(\frac{w}{h}\right)^2 \quad \text{(Eq. 15c)}$$

where w= the flat width of flange

h= the flat width of web

ψ= (Eq. 14b)

Eq. 15a shows the correlation between buckling coefficient, k, and the ratio of compression and tension stresses on the top and bottom of web, whereas Eq. 16b represents the relationship between buckling coefficient, k, and the ratio of flat widths of flange and web. The ratio of compression and tension stresses in the web and the ratio of widths of flange and web, the theoretical coefficient, k, is represented by Fig. 16c.

Method VI: $M_{uc,d} = F_y\ S_{ex,Fk}$

For each test specimen, the computed moment capacity was evaluated by using the following equation:

$$M_{uc,d} = F_y\ S_{ex,Fk} \qquad \text{(Eq. 16)}$$

where $S_{ex,Fk}$ is the effective section modulus evaluated at F_y using each proposed web buckling coefficient (Eqs. 15a, 15b or 15c).

Tables 14-1, 14-2 and 14-3 show the tested moment, computed moment and the ratio of tested moment and computed moment for the three test sequences. Based on Eq. 15b for evaluating the buckling coefficient, the three test sequences have good correlation between tested moment and computed ultimate bending moment. Table 14-4 summaries the results in Tables 14-1, 14-2 and 14-3. By using Eq. 15b, Table 14-4 indicates that satisfactory results were obtained for the tested and computed moment capacities having a mean value of 1.023 for test sequence No. 1, 1.006 for test sequence No. 2, 0.998 for test sequence No. 3 and 1.005 for the three test sequences. A study of Table 14-4 reveals that the primary parameter effecting distortional buckling behaviour is the w/h ratio. It seems reasonable that there is some correlation between the flat widths of flanges and web when the test specimens undergo a mode of distortional buckling as discussed above (Model A).

ROTATIONAL STIFFNESS

A study was also undertaken to investigate the distortional buckling load (P_{cr}) and rotational stiffness (k_ϕ). According to the analysis shown in Tables 10-4 and 12-4, the rotational restraint, k_ϕ, defined by Eq. 8b is the best expression to explain the distortional buckling behaviour. Using Eq. 8a to determine the rotational restraint, k_ϕ, underestimates the moment capacity, and using Eq. 8c to define the rotational stiffness, k_ϕ, overestimates the moment capacity. Therefore, a possible design modification employing Eq. 8b has been developed. Figure 15 shows the correlation between P_{cr} and k_ϕ for the test specimens. Based on the regression analysis, the following relationship was derived:

$$P_{cr}=1.970+516.7465k_\phi^2-979.5711k_\phi^3 \qquad \text{(Eq. 17)}$$

where P_{cr}= the distortional buckling load for the gross section area of the flange and edge stiffener as defined in mode A

k_ϕ= the stiffness of rotational restraint

E= modulus of elasticity of steel (29500 ksi)

The ultimate moment capacity, $M_{uc,d}$, was computed by the following equation:

$$M_{uc,d}= F_{d,p}\ S_{ex,p} \qquad \text{(Eq. 18)}$$

where $\sigma_d= P_{cr}/A$

P_{cr}= Eq. 17

A= the gross section area of the flange and edge stiffener

$F_{d,p}$= Eq. 8

$S_{ex,p}$= the effective section modulus using AISI effective width equations evaluated at $F_{d,p}$.

Method VII: $M_{uc,d}= F_{d,p}\ S_{ex,p}$

The computed moments capacity based on Eq. 18 are shown in Tables 15-1, 15-2 and 15-3 which present the solution using the more rigourous calculation procedure (previously presented in Table 9-1). Table 15-4 summarizes the results and shows the comparison of Method I and Method VII.

SUMMARY

To obtain the objective of this investigation, which was to study the flexural behavior of C-shaped members with or without web openings subjected to a pure bending moment, a total of 68 beam specimen tests have been evaluated. Fifty-one beam specimens were conducted at UMR and 17 tests were conducted at the University of Waterloo. There are 14 beam specimens failed by distortional buckling at UMR and all the 17 tests at the University of Waterloo had distortional buckling failures. Based on the study reported herein, the following tentative conclusions can be drawn:

(1) The current AISI Specification (Method I) did not accurately estimate the bending strength for all of the C-sections having a web punchout included in this test program.

(2) This study indicates that for test specimens governed by local buckling the main parameter to influence the bending capacity of a member with a web punchout is the ratio of a/h.

(3) For specimens whose failure was attributed to local buckling Methods I and III employ the concept of an effective web depth. Method I overestimates the moment capacity for the a/h ratio of 0.47 and 0.74, whereas method III satisfactorily predicts the bending strength for all test specimens. Method II overestimates the moment capacity for specimens having a a/h ratio of 0.47.

(4) In the analysis presented in Tables 12-1, 12-2 and 12-3, the model B is not a good model to account for the distortional buckling behavior for C-channel sections. This model was developed for panel sections and the assumptions, that distortional buckling occurs before local buckling and no lateral displacement is allowed at the web and tension flange junction, are not suitable for the three test sequences in this study.

(5) The results from the experiment and numerical analysis of test specimens failing by distortional buckling, indicate that model A is a good approximation for determining the strength of beams with slender webs.

(6) More tests will be conducted to develop an equation for estimating the rotational stiffness and explain the distortional

buckling behavior using model A.

(7) Studies to date indicate that the parameters w/h and f_2/f_1 influence the distortional buckling behavior.

(8) From the results of 39 beam tests shown in Tables 4-1, 4-2 and 4-3, the comparison of the moment ratio of test to computed moment and w/h is presented graphically by Fig. 16 for the three sequences, which indicates that a critical value of w/h needs to be developed to determine whether a beam member is controlled by either local buckling or distortional buckling behaviour.

(9) Two simplified approaches for evaluating the ultimate bending moment for beam members having a deep web, narrow flanges and small lips which undergo the distortional buckling behaviour has been developed. Additional tests will be conducted to confirm and refine these analytical models (Method VI and VII).

REFERENCES

1. Batson, K.D., LaBoube, R.A., and Yu, W.W., "Flexural Behavior of Web Elements with Openings," First Progress Report, Department of Civil Engineering, University of Missouri-Rolla, Rolla, MO, Feburary 7, 1991
2. Batson, K.D., LaBoube, R.A., and Yu, W.W., "Flexural Behavior of Web Elements with Openings," Second Progress Report, Department of Civil Engineering, University of Missouri-Rolla, Rolla, MO, June 7, 1991
3. Shan, M.Y., Batson, K.D., LaBoube, R.A., and Yu, W.W., "Flexural

Behavior of Web Elements with Openings," Third Progress Report, Department of Civil Engineering, University of Missouri-Rolla, Rolla, MO, October 15, 1991

4. Shan, M.Y., Batson, K.D., LaBoube, R.A., and Yu, W.W., "Flexural Behavior of Web Elements with Openings," Fourth Progress Report, Department of Civil Engineering, University of Missouri-Rolla, Rolla, MO, January 15, 1992

5. Schuster, R.M., "Testing of Perforated C-Stud Sections in Bending", University of Waterloo, Ontario, Canada, March, 1992

6. Hancock, G.J., "Distortional Buckling of Steel Storage Rack Columns", Journal of Structural Engineering, ASCE, 111(12), 2770-2783, 1985

7. Lau, S.C.W., and Hancock, G.J., "Distortional Buckling Formulas for Channel Columns", Journal of Structural Engineering, ASCE Vol. 113, No. 5, May, 1987

8. Lundquist, E.E., Stowell, E.Z., and Schuette, E.H., "Principles of Moment Distribution Applied to Stability of Structures Composed of Bars or Plates", NACA Wartime Report L-326, 1943

9. Lau, S.C.W., and Hancock, G.J., "Distortional Buckling Formulae for Thin-Walled Channel Columns", Research Report No. R521, School of Civil and Mining Engineering, University of Sydney, Sydney, Australia, 1986

10. Charnvarnichborikarn, P., "Distortional Buckling of Cold-Formed Steel Z-Sections", University of Manitoba, April, 1992

11. Kwon, Y.B., and Hancock, G.J., "Tests of Cold-Formed Channels with Local and Distortional Buckling", Journal of Structural

Engineering, ASCE Vol. 117, No. 7, July, 1992

12. Serrette, R., and Pekoz, T., "Cold-Formed Steel Panels with Laterally Unsupported Compression Flanges", Cornell University, September, 1991

13. Serrette, R., and Pekoz, T., "Local and Distortional Buckling of Thin-Walled Beams", Eleventh International Specialty Conference on Cold-Formed Steel Structures, St. Louis, MO October, 1992

14. "Cold-Formed Steel Design Manual", American Iron and Steel Institute, August 19, 1986, with December 11, 1989 Addendum.

15. LaBoube, R.A., and Yu, W.W., "Structural Behavior of Beam Webs Subjected to Bending Stress", Department of Civil Engineering, University of Missouri-Rolla, Rolla, MO, June, 1978

NOTATION

Model A:

A= gross section area
b= flat width of compression element
b_e= effective flat width of compression element
b_f= width of flange
b_w= width of web
D= plate flexure rigidity per unit width
E= Young's modulus
F_d= nominal elastic or inelastic distortional buckling stress
F_y= yield stress of steel
G= shear modulus
h_x, h_y= x,y coordinates of flange and web junction
I_o= polar second moment of area about the shear center
I_x, I_y= second moments of area flange about the x,y axes
I_{xy}= product second moment of area of flange about x,y axes
I_w= warping constant of flange
J= torsion constant of flange
k= stress coefficient
k_x, k_ϕ= stiffness of laternal and rotational restraints

P_{cr}= critical buckling load
Q_y= intensity of reaction force along the elastic support acting in the y-direction
t= thickness
u,v,ϕ= deflections in the x,y directions and angle of rotation
x_o,y_o= x,y coordinates of the shear center
λ= buckling half-wavelength
σ_b= distortional buckling stress

Model b:

β_1= geometric parameter
C_w= warping constant
k_l= effective length factor
k_y= linear elastic extensional spring constant
k_ϕ= linear elastic rotational spring constant
L_e= equivalent unsupported length of the leg
L_u= clear unsupported span length
ν= Poisson's ratio
w_f=width of the tension flange
w_w= depth of the web in the leg under consideration
γ= ratio of the elastic local buckling stress in the web to the buckling stress required for the web to be fully effective

TABLE 1-1
DIMENSIONS OF TEST SPECIMENS
UMR TEST SEQUENCE No. 1

Beam Specimen No.	Cross-Section Dimenisions (inches)											Hole Geom. (in.)	
	Thick.	D1	D2	B1	B2	B3	B4	d1	d2	d3	d4	b	a
2,16,1&2(H)	0.062	2.51	2.51	1.61	1.61	1.63	1.61	0.40	0.45	0.42	0.43	2	0.75
2,20,1&2(H)	0.039	2.50	2.48	1.60	1.60	1.60	1.60	0.42	0.41	0.42	0.41	2	0.75
2,20,3&4(H)	0.039	2.51	2.52	1.59	1.62	1.58	1.60	0.36	0.42	0.47	0.41	2	0.75
3,14,1&2(H)	0.077	3.68	3.68	1.65	1.64	1.63	1.63	0.57	0.55	0.56	0.52	4	1.5
3,14,3&4(H)	0.077	3.69	3.69	1.63	1.62	1.64	1.63	0.53	0.53	0.62	0.55	4	1.5
3,18,1&2(H)	0.044	3.75	3.65	1.56	1.56	1.57	1.58	0.58	0.56	0.58	0.54	4	1.5
3,18,3&4(H)	0.044	3.65	3.64	1.56	1.58	1.56	1.57	0.56	0.57	0.54	0.54	4	1.5
3,20,1&2(H)	0.044	3.65	3.71	1.56	1.64	1.55	1.59	0.52	0.56	0.55	0.56	4	1.5
3,20,3&4(H)	0.044	3.67	3.69	1.56	1.59	1.55	1.61	0.60	0.56	0.52	0.59	4	1.5
12,14,1&2(H)	0.098	12.08	12.07	1.64	1.63	1.69	1.63	0.69	0.60	0.60	0.62	4	1.5
12,14,3&4(H)	0.098	12.05	12.00	1.64	1.60	1.67	1.71	0.65	0.64	0.65	0.64	4	1.5
12,16,1&2(H)	0.055	11.96	11.97	1.57	1.57	1.57	1.56	0.50	0.61	0.52	0.43	4	1.5
12,16,3&4(H)	0.055	12.07	11.96	1.56	1.57	1.57	1.58	0.42	0.53	0.58	0.53	4	1.5

Note: See Fig. 2 for the symbols used for dimensions.
See Fig. 1 for the symbols used for the hole geometry.
Specimen Designation: 12,14,1&2(H)
12-Nominal Depth
14-Gage Number
1&2-Individual Cross Section
(H)-Web Opening
(N)-No Web Opening

TABLE 1-2
DIMENSIONS OF TEST SPECIMENS
UMR TEST SEQUENCE NO. 2

Beam Specimen No.	Cross-Section Dimensions (inches)											Hole Geom. (in.)	
	Thick.	D1	D2	B1	B2	B3	B4	d1	d2	d3	d4	b	a
2,16,1&2(H)	0.059	2.46	2.46	1.62	1.63	1.62	1.61	0.47	0.46	0.51	0.51	4.0	1.5
2,16,3&4(H)	0.059	2.47	2.46	1.63	1.62	1.62	1.63	0.47	0.52	0.52	0.46	4.0	1.5
2,16,1&2(N)	0.057	2.48	2.48	1.62	1.63	1.61	1.61	0.45	0.45	0.51	0.51		
2,16,3&4(N)	0.057	2.48	2.48	1.61	1.63	1.63	1.61	0.51	0.46	0.47	0.51		
2,20,1&2(H)	0.033	2.42	2.42	1.63	1.64	1.63	1.62	0.42	0.42	0.50	0.50	4.0	1.5
2,20,3&4(H)	0.033	2.42	2.43	1.63	1.64	1.63	1.62	0.42	0.41	0.50	0.50	4.0	1.5
2,20,1&2(N)	0.033	2.44	2.44	1.63	1.64	1.63	1.62	0.41	0.40	0.49	0.50		
2,20,3&4(N)	0.033	2.46	2.45	1.63	1.63	1.61	1.61	0.39	0.40	0.52	0.51		
3,14,1&2(H)	0.071	3.65	3.62	1.62	1.66	1.63	1.63	0.54	0.55	0.49	0.50	4.0	1.5
3,14,3&4(H)	0.071	3.64	3.63	1.63	1.62	1.62	1.63	0.54	0.47	0.49	0.54	4.0	1.5
3,18,1&2(H)	0.044	3.61	3.63	1.61	1.65	1.65	1.62	0.51	0.52	0.50	0.50	4.0	1.5
3,18,3&4(H)	0.044	3.62	3.63	1.62	1.66	1.65	1.64	0.50	0.50	0.52	0.52	4.0	1.5
3,18,1&2(N)	0.044	3.66	3.68	1.66	1.61	1.62	1.66	0.52	0.47	0.47	0.52		
3,18,3&4(N)	0.044	3.64	3.64	1.66	1.64	1.65	1.63	0.49	0.49	0.50	0.48		
3,20,1&2(H)	0.036	3.61	3.60	1.63	1.62	1.63	1.62	0.46	0.47	0.46	0.47	4.0	1.5
3,20,3&4(H)	0.036	3.61	3.61	1.64	1.63	1.64	1.63	0.46	0.47	0.47	0.47	4.0	1.5
3,20,5&6(H)	0.036	3.60	3.60	1.63	1.63	1.62	1.63	0.46	0.46	0.46	0.47	4.0	1.5
3,20,1&2(N)	0.035	3.60	3.60	1.63	1.62	1.63	1.63	0.47	0.47	0.46	0.46		
3,20,3&4(N)	0.035	3.60	3.60	1.63	1.63	1.63	1.63	0.48	0.46	0.46	0.47		
3,20,5&6(N)	0.035	3.59	3.60	1.63	1.62	1.62	1.62	0.47	0.47	0.47	0.46		

TABLE 1-2 (CONTINUED)
DIMENSIONS OF TEST SPECIMENS
UMR TEST SEQUENCE No. 2

Beam Specimen No.	Cross-Section Dimensions(inches)											Hole Geom. (in.)	
	Thick.	D1	D2	B1	B2	B3	B4	d1	d2	d3	d4	b	a
6A,18,1&2(H)	0.046	6.06	6.05	1.62	1.62	1.55	1.55	0.47	0.47	0.50	0.50	4.0	1.5
6A,18,3&4(H)	0.046	6.05	6.02	1.62	1.62	1.55	1.55	0.47	0.48	0.50	0.51	4.0	1.5
6B,18,1&2(H)	0.048	5.96	5.96	1.98	1.99	1.98	1.99	0.64	0.59	0.59	0.64	4.0	1.5
6B,18,3&4(H)	0.048	5.95	5.98	1.97	1.98	1.99	1.98	0.60	0.65	0.64	0.63	4.0	1.5
6C,18,1&2(H)	0.046	6.02	6.02	2.42	2.43	2.43	2.43	0.70	0.62	0.62	0.70	4.0	1.5
6C,18,3&4(H)	0.046	6.02	6.02	2.43	2.43	2.43	2.43	0.70	0.70	0.61	0.62	4.0	1.5
6,20,1&2(H)	0.033	5.92	5.92	1.63	1.62	1.52	1.53	0.44	0.47	0.44	0.42	4.0	1.5
8,18,1&2(H)	0.045	7.95	7.94	1.59	1.58	1.58	1.58	0.47	0.47	0.48	0.47	4.0	1.5
8C,18,1&2(H)	0.046	8.00	8.00	2.42	2.45	2.44	2.43	0.61	0.69	0.69	0.62	4.0	1.5
8C,18,3&4(H)	0.046	8.00	8.00	2.42	2.45	2.45	2.43	0.60	0.70	0.70	0.60	4.0	1.5
12,16,1&2(H)	0.060	11.95	11.95	1.63	1.63	1.63	1.63	0.53	0.54	0.52	0.53	4.0	1.5
12,16,3&4(H)	0.060	11.98	12.02	1.63	1.63	1.62	1.63	0.47	0.50	0.55	0.53	4.0	1.5
12,16,5&6(H)	0.060	11.96	11.97	1.63	1.63	1.63	1.63	0.51	0.50	0.51	0.52	4.0	1.5
12,16,7&8(H)	0.060	11.97	11.96	1.63	1.63	1.62	1.63	0.48	0.55	0.56	0.49	4.0	1.5
12,16,1&2(N)	0.062	11.95	11.94	1.63	1.63	1.63	1.63	0.51	0.55	0.54	0.48		
12,16,3&4(N)	0.062	11.96	11.98	1.64	1.63	1.63	1.63	0.46	0.55	0.56	0.49		

Note: Specimen Designation: 6A,18,1&2(H)
6-Nominal Depth
A-Type of Flange Width
18-Gage Number
1&2-Individual Cross Section
(H)-Web Opening
(N)-No Web Opening

TABLE 1-3
DIMENSIONS OF TEST SPECIMENS
SCHUSTER TEST SEQUENCE No. 3

Beam Specimen No.	Cross-Section Dimenisions (inches)											Hole Geom. (in.)	
	Thick.	D1	D2	B1	B2	B3	B4	d1	d2	d3	d4	b	a
BS1	0.048	7.99	7.99	1.61	1.61	1.61	1.61	0.47	0.47	0.47	0.47		
BS2	0.048	7.99	7.99	1.61	1.61	1.61	1.61	0.47	0.47	0.47	0.47		
BP4-40	0.047	7.99	7.99	1.61	1.61	1.61	1.61	0.47	0.47	0.47	0.47	4.02	1.50
BP5-40	0.047	7.99	7.99	1.61	1.61	1.61	1.61	0.47	0.47	0.47	0.47	4.02	1.50
BP6-40	0.047	7.99	7.99	1.61	1.61	1.61	1.61	0.47	0.47	0.47	0.47	4.02	1.50
BP7-65	0.047	7.99	7.99	1.58	1.58	1.58	1.58	0.47	0.47	0.47	0.47	4.53	2.48
BP8-65	0.047	7.99	7.99	1.61	1.58	1.61	1.58	0.47	0.47	0.47	0.47	4.53	2.48
BP9-65	0.047	7.99	7.99	1.61	1.58	1.58	1.58	0.47	0.47	0.47	0.47	4.53	2.48
CS1	0.048	7.99	7.99	1.58	1.58	1.58	1.58	0.51	0.51	0.51	0.51		
CS2	0.048	8.03	7.99	1.58	1.58	1.58	1.58	0.51	0.51	0.51	0.51		
CS3	0.048	8.03	7.99	1.61	1.58	1.58	1.58	0.51	0.51	0.51	0.51		
CP4-40	0.048	7.99	7.99	1.58	1.58	1.58	1.58	0.51	0.51	0.51	0.51	4.65	1.69
CP5-40	0.048	7.99	7.99	1.58	1.61	1.58	1.58	0.51	0.51	0.51	0.51	4.65	1.69
CP6-40	0.048	8.03	8.03	1.61	1.61	1.58	1.58	0.51	0.51	0.51	0.51	4.65	1.69
CP7-65	0.048	7.99	7.99	1.61	1.61	1.61	1.61	0.51	0.51	0.51	0.51	4.61	2.52
CP8-65	0.048	8.03	7.99	1.58	1.61	1.58	1.61	0.51	0.51	0.51	0.51	4.61	2.52
CP9-65	0.048	7.99	7.99	1.61	1.61	1.61	1.61	0.51	0.51	0.51	0.51	4.61	2.52

Note: Specimen Designation: BP4-40
B-Section Type
P-Perforated Web
4-Test No.
40-Depth of Perforation in mm

TABLE 2-1
MATERIAL PROPERTIES
UMR TEST SEQUENCE No. 1

Specimen No.	Thickness (in.)	F_y (ksi)	F_u (ksi)	Elongation (%)
2,16(H)	0.062	37	49	38
2,20(H)	0.039	34	48	44
3,14(H)	0.077	64	78	23
3,18(H)	0.044	47	60	31
3,20(H)	0.044	47	60	31
12,14(H)	0.098	36	47	35
12,16(H)	0.055	49	57	32

TABLE 2-2
MATERIAL PROPERTIES
UMR TEST SEQUENCE NO. 2

Specimen No.	Thickness (in.)	F_y (ksi)	F_u (ksi)	Elongation (%)
2,16(H)	0.059	54	75	39
2,16(N)	0.057	58	78	36
2,20(H)	0.033	67	72	35
2,20(N)	0.033	65	75	33
3,14(H)	0.071	81	104	22
3,14(N)	0.076	52	110	20
3,18(H)	0.044	53	70	24
3,18(N)	0.044	63	81	14
3,20(H)	0.036	64	79	29
3,20(N)	0.035	61	82	33
6A,18(H)	0.046	47	67	41
6B,18(H)	0.048	75	83	16
6C,18(H)	0.046	31	55	55
6,20(H)	0.033	93	97	5
8,18(H)	0.045	72	74	30
8C,18(H)	0.046	22	59	55
12,16(H)	0.060	61	75	38
12,16(N)	0.062	62	74	38

TABLE 2-3
MATERIAL PROPERTIES
SCHUSTER TEST SEQUENCE No. 3

Specimen No.	Thickness (in.)	F_y (ksi)	F_u (ksi)	Elongation (%)
BS	0.047	39	52	31
BP	0.047	39	51	31
CS	0.048	48	52	36
CP	0.047	49	52	36

TABLE 3-1
TEST RESULTS
UMR TEST SEQUENCE No. 1

Beam Specimen No.	Span Length (ft)	x (in.)	P (kips)
2,16,1&2(H)	12.5	39	1.04
2,20,1&2(H)	12.5	39	0.46
2,20,3&4(H)	12.5	39	0.46
3,14,1&2(H)	12.5	39	3.70
3,14,3&4(H)	12.5	39	3.54
3,18,1&2(H)	12.5	39	1.35
3,18,3&4(H)	12.5	39	1.37
3,20,1&2(H)	12.5	39	1.35
3,20,3&4(H)	12.5	39	1.43
12,14,1&2(H)	16	60	7.16
12,14,3&4(H)	16	60	7.50
12,14,5&6(H)	16	60	7.95
12,14,7&8(H)	16	60	7.98
12,16,1&2(H)	16	60	4.38
12,16,3&4(H)	16	60	4.79

TABLE 3-2
TEST RESULTS
UMR TEST SEQUENCE No. 2

Beam Specimen No.	Span Length (ft)	x (in.)	P (kips)
2,16,1&2(H)	12.5	39	1.35
2,16,3&4(H)	12.5	39	1.36
2,16,1&2(N)	12.5	39	1.59
2,16,3&4(N)	12.5	39	1.62
2,20,1&2(H)	12.5	39	0.60
2,20,3&4(H)	12.5	39	0.64
2,20,1&2(N)	12.5	39	0.77
2,20,3&4(N)	12.5	39	0.76
3,14,1&2(H)	12.5	39	4.31
3,14,3&4(H)	12.5	39	4.26
3,18,1&2(H)	12.5	39	1.60
3,18,3&4(H)	12.5	39	1.51
3,18,1&2(N)	12.5	39	2.44
3,18,3&4(N)	12.5	39	2.15
3,20,1&2(H)	12.5	39	1.20
3,20,3&4(H)	12.5	39	1.10
3,20,5&6(H)	12.5	39	1.34
3,20,1&2(N)	12.5	39	1.17
3,20,3&4(N)	12.5	39	1.26
3,20,5&6(N)	12.5	39	1.41
6A,18,1&2(H)	16	60	1.64
6A,18,3&4(H)	16	60	1.70
6B,18,1&2(H)	16	60	3.43
6B,18,3&4(H)	16	60	3.45
6C,18,1&2(H)	16	60	1.67
6C,18,3&4(H)	16	60	1.70
6,20,1&2(H)	16	60	1.15
8,18,1&2(H)	16	60	2.76
8C,18,1&2(H)	16	60	2.10
8C,18,3&4(H)	16	60	1.84
12,16,1&2(H)	16	60	6.49
12,16,3&4(H)	16	60	6.44
12,16,5&6(H)	16	60	6.39
12,16,7&8(H)	16	60	6.67
12,16,1&2(N)	16	60	6.50
12,16,3&4(N)	16	60	6.76

TABLE 3-3
TEST RESULTS
SCHUSTER TEST SEQUENCE No. 3

Beam Specimen No.	Span Length (ft)	x (in.)	P (kips)
BS1	14	72	3.12
BS2	14	72	3.18
BP4-40	14	72	3.16
BP5-40	14	72	3.07
BP6-40	14	72	3.18
BP7-65	14	72	3.14
BP8-65	14	72	3.18
BP9-65	14	72	3.18
CS1	14	72	3.34
CS2	14	72	3.34
CS3	14	72	3.43
CP4-40	14	72	3.45
CP5-40	14	72	3.28
CP6-40	14	72	3.47
CP7-65	14	72	3.44
CP8-65	14	72	3.41
CP9-65	14	72	3.40

TABLE 4-1
COMPARISON OF TEST RESULTS
(Based on 1986 AISI Specification)
UMR TEST SEQUENCE No. 1

Beam Specimen No.	h/t	a/h	M_{ut} (k-in.)	M_{uc} (k-in.)	$(M_{ut})/(M_{uc})$
2,16,1&2(H)	33	0.36	23.37	22.35	1.046
2,20,1&2(H)	54	0.36	11.85	12.51	0.947
2,20,3&4(H)	54	0.35	11.95	12.04	0.993
Mean					0.995
Standard Deviation					0.0495
3,14,1&2(H)	42	0.47	75.17	82.30	0.913
3,14,3&4(H)	42	0.47	72.01	81.02	0.889
3,18,1&2(H)	75	0.45	29.32	33.93	0.864
3,18,3&4(H)	74	0.46	29.70	33.93	0.875
3,20,1&2(H)	74	0.46	29.31	33.84	0.866
3,20,3&4(H)	74	0.46	30.78	33.46	0.920
Mean					0.888
Standard Deviation					0.0240
12,14,1&2(H)	118	0.13	219.52	323.42	0.679
12,14,3&4(H)	118	0.13	229.87	326.30	0.704
12,14,5&6(H)	118	0.13	243.37	323.64	0.752
12,14,7&8(H)	118	0.13	244.27	320.54	0.762
12,16,1&2(H)	210	0.13	135.97	181.89	0.748
12,16,3&4(H)	211	0.13	148.27	182.18	0.814
Mean					0.743
Standard Deviation					0.0472

TABLE 4-2
COMPARISON OF TEST RESULTS
(Based on 1986 AISI Specification)
UMR TEST SEQUENCE No. 2

Beam Specimen No.	h/t	a/h	M_{ut} (k-in.)	M_{uc} (k-in.)	$(M_{ut})/(M_{uc})$ (H)	$(M_{ut})/(M_{uc})$ (N)
2,16,1&2(H)	34	0.74	29.17	29.90	0.976	
2,16,3&4(H)	35	0.74	29.47	30.23	0.975	
2,16,1&2(N)	36		33.85	31.09		1.089
2,16,3&4(N)	36		34.54	31.32		1.103
2,20,1&2(H)	62	0.73	14.65	17.19	0.852	
2,20,3&4(H)	62	0.73	15.33	17.19	0.892	
2,20,1&2(N)	63		17.96	16.56		1.085
2,20,3&4(N)	63		17.77	16.69		1.065
Mean					0.924	1.086
Standard Deviation					0.0619	0.0157
3,14,1&2(H)	45	0.47	86.99	89.50	0.972	
3,14,3&4(H)	45	0.47	85.68	88.68	0.966	
3,18,1&2(H)	73	0.47	34.15	34.85	0.980	
3,18,3&4(H)	73	0.47	32.39	35.07	0.924	
3,18,1&2(N)	74		50.53	39.28		1.286
3,18,3&4(N)	74		44.87	39.28		1.142
3,20,1&2(H)	90	0.47	26.35	31.86	0.827	
3,20,3&4(H)	90	0.47	24.40	31.73	(0.769)	
3,20,5&6(H)	90	0.47	28.88	31.60	0.914	
3,20,1&2(N)	92		25.76	29.50		(0.873)
3,20,3&4(N)	92		27.42	29.62		0.926
3,20,5&6(N)	92		30.34	29.50		1.028
Mean					0.931	1.096
Mean					(0.907)*	(1.051)*
Standard Deviation					0.0574	0.1546
Standard Deviation					(0.0804)*	(0.1668)*

* Includes Beam Specimen Nos. 3,20,3&4(H) and 3,20,1&2(N)

TABLE 4-2 (CONTINUED)
COMPARISON OF TEST RESULTS
(Based on 1986 AISI Specification)
UMR TEST SEQUENCE No. 2

Beam Specimen No.	h/t	a/h	M_{ut} (k-in.)	M_{uc} (k-in.)	$(M_{ut})/(M_{uc})$ (H)	(N)
6A,18,1&2(H)	123	0.27	53.58	67.59	0.793	
6A,18,3&4(H)	122	0.27	55.38	67.68	0.818	
6B,18,1&2(H)	116	0.27	107.13	106.92	1.002	
6B,18,3&4(H)	116	0.27	107.73	107.67	1.001	
6C,18,1&2(H)	122	0.27	54.48	56.12	0.971	
6C,18,3&4(H)	122	0.27	55.38	55.81	0.992	
6,20,1&2(H)	168	0.27	38.88	60.08	(0.647)	
Mean					0.930	
Mean					(0.889)*	
Standard Deviation					0.0970	
Standard Deviation					(0.1387)*	
8,18,1&2(H)	168	0.20	87.18	112.61	(0.774)	
8C,18,1&2(H)	165	0.20	67.38	63.01	1.069	
8C,18,3&4(H)	165	0.20	59.58	62.52	0.953	
Mean					1.011	
Mean					(0.932)**	
Standard Deviation					0.0820	
Standard Deviation					(0.1486)**	
12,16,1&2(H)	192	0.13	198.93	255.17	0.780	
12,16,3&4(H)	192	0.13	197.52	248.50	0.795	
12,16,5&6(H)	192	0.13	195.93	251.17	0.780	
12,16,7&8(H)	192	0.13	204.33	249.23	0.820	
12,16,1&2(N)	186		199.38	264.18		0.755
12,16,3&4(N)	186		207.03	262.83		0.788
Mean					0.794	0.772
Standard Deviation					0.0189	0.0233

* Includes Beam Specimen No. 6,20,1&2(H)

** Includes Beam Specimen No. 8,18,1&2(H)

TABLE 4-3
COMPARISON OF TEST RESULTS
(Based on 1986 AISI Specification)
SCHUSTER TEST SEQUENCE No. 3

Beam Specimen No.	h/t	a/h	M_{ut} (k-in.)	M_{uc} (k-in.)	$(M_{ut})/(M_{uc})$ (H)	$(M_{ut})/(M_{uc})$ (N)
BS1	162		74.88	90.86		0.824
BS2	162		76.21	90.86		0.839
Mean						0.832
BP4-40	163	0.19	75.85	89.16	0.851	
BP5-40	163	0.19	73.64	89.16	0.826	
BP6-40	163	0.19	76.21	89.16	0.855	
Mean					0.844	
BP7-65	163	0.32	75.23	89.08	0.845	
BP8-65	163	0.32	76.38	89.08	0.857	
BP9-65	163	0.32	76.21	89.16	0.855	
Mean					0.852	
CS1	161		80.10	105.98		0.756
CS2	161		80.10	105.98		0.756
CS3	161		82.22	105.98		0.776
Mean						0.763
CP4-40	162	0.22	82.84	104.86	0.790	
CP5-40	162	0.22	78.68	104.86	0.750	
CP6-40	163	0.22	83.37	104.17	0.800	
Mean					0.780	
CP7-65	162	0.33	81.69	103.68	0.788	
CP8-65	163	0.33	81.78	104.86	0.780	
CP9-65	162	0.33	81.87	103.68	0.790	
Mean					0.786	

TABLE 5-1
COMPARISON OF TEST RESULTS
(Based on 1986 AISI Specification, b_2=0.0)
UMR TEST SEQUENCE No. 1

Beam Specimen No.	h/t	a/h	M_{ut} (k-in)	M_{uc} (k-in)	$(M_{ut})/(M_{uc})$
2,16,1&2(H)	33	0.36	23.37	17.02	1.373
2,20,1&2(H)	54	0.36	11.85	11.90	0.996
2,20,3&4(H)	54	0.35	11.95	11.90	1.004
Mean					1.124
Standard Deviation					0.2154
3,14,1&2(H)	42	0.47	75.17	80.13	0.938
3,14,3&4(H)	42	0.47	72.01	75.90	0.949
3,18,1&2(H)	75	0.45	29.32	32.99	0.889
3,18,3&4(H)	74	0.46	29.70	32.90	0.903
3,20,1&2(H)	74	0.46	29.31	33.18	0.883
3,20,3&4(H)	74	0.46	30.78	31.58	0.975
Mean					0.923
Standard Deviation					0.0368

TABLE 5-2
COMPARISON OF TEST RESULTS
(Based on 1986 AISI Specification, b_2=0.0)
UMR TEST SEQUENCE No. 2

Beam Specimen No.	h/t	a/h	M_{ut} (k-in)	M_{uc} (k-in)	$(M_{ut})/(M_{uc})$
2,16,1&2(H)	34	0.74	29.17	28.35	1.029
2,16,3&4(H)	35	0.74	29.47	28.61	1.030
2,20,1&2(H)	62	0.73	14.65	16.34	0.897
2,20,3&4(H)	62	0.73	15.33	16.33	0.939
Mean					0.974
Standard Deviation					0.0666
3,14,1&2(H)	45	0.47	86.99	87.00	1.000
3,14,3&4(H)	45	0.47	85.68	83.27	1.029
3,18,1&2(H)	73	0.47	34.15	33.36	1.024
3,18,3&4(H)	73	0.47	32.39	33.07	0.979
3,20,1&2(H)	90	0.47	26.35	29.14	0.904
3,20,3&4(H)	90	0.47	24.40	29.04	(0.840)
3,20,5&6(H)	90	0.47	28.88	28.98	0.997
Mean					0.989
Mean					(0.968)*
Standard Deviation					0.0455
Standard Deviation					(0.0699)*

* Includes Beam Specimen No. 3,20,3&4(H)

TABLE 6-1
COMPARISON OF TEST RESULTS
(Based on Net Section Approach)
UMR TEST SEQUENCE No. 1

Beam Specimen No.	h/t	a/h	M_{ut} (k-in)	M_{ufn} (k-in)	$(M_{ut})/(M_{ufn})$
2,16,1&2(H)	33	0.36	23.37	22.05	1.060
2,20,1&2(H)	54	0.36	11.85	12.14	0.976
2,20,3&4(H)	54	0.35	11.95	11.65	1.026
Mean					1.021
Standard Deviation					0.0423
3,14,1&2(H)	42	0.47	75.17	81.98	0.917
3,14,3&4(H)	42	0.47	72.01	73.42	0.981
3,18,1&2(H)	75	0.45	29.32	33.81	0.867
3,18,3&4(H)	74	0.46	29.70	33.77	0.879
3,20,1&2(H)	74	0.46	29.31	32.34	0.906
3,20,3&4(H)	74	0.46	30.78	34.08	0.903
Mean					0.909
Standard Deviation					0.0399

Note: M_{ut} = Tested moment capacities
M_{ufn} = Moment capacity based on the net section

TABLE 6-2
COMPARISON OF TEST RESULTS
(Based on Net Section Approach)
UMR TEST SEQUENCE No. 2

Beam Specimen No.	h/t	a/h	M_{ut} (k-in)	M_{ufn} (k-in)	$(M_{ut})/(M_{ufn})$
2,16,1&2(H)	34	0.74	29.17	27.09	1.077
2,16,3&4(H)	35	0.74	29.47	27.45	1.074
2,20,1&2(H)	62	0.73	14.65	13.52	1.084
2,20,3&4(H)	62	0.73	15.33	13.50	1.136
Mean					1.093
Standard Deviation					0.0291
3,14,1&2(H)	45	0.47	86.99	88.82	0.979
3,14,3&4(H)	45	0.47	85.68	84.77	1.011
3,18,1&2(H)	73	0.47	34.15	33.79	1.011
3,18,3&4(H)	73	0.47	32.39	33.48	0.967
3,20,1&2(H)	90	0.47	26.35	30.06	0.877
3,20,3&4(H)	90	0.47	24.40	30.11	(0.810)
3,20,5&6(H)	90	0.47	28.88	29.94	0.965
Mean					0.968
Mean					(0.946)*
Standard Deviation					0.0492
Standard Deviation					(0.0748)*

See Table 6-1 for Notes

* Includes Beam Specimen No. 3,20,3&4(H)

TABLE 7-1
COMPARISON OF TEST RESULTS
(Based on Effective Net Section Approach)
UMR TEST SEQUENCE No. 1

Beam Specimen No.	h/t	a/h	M_{ut} (k-in)	M_{uen} (k-in)	$(M_{ut})/(M_{uen})$
2,16,1&2(H)	33	0.36	23.37	22.05	1.060
2,20,1&2(H)	54	0.36	11.85	11.97	0.990
2,20,3&4(H)	54	0.35	11.95	11.45	1.044
Mean					1.031
Standard Deviation					0.0367
3,14,1&2(H)	42	0.47	75.17	81.02	0.928
3,14,3&4(H)	42	0.47	72.01	72.02	1.000
3,18,1&2(H)	75	0.45	29.32	32.29	0.908
3,18,3&4(H)	74	0.46	29.70	32.26	0.921
3,20,1&2(H)	74	0.46	29.31	30.79	0.952
3,20,3&4(H)	74	0.46	30.78	32.44	0.949
Mean					0.943
Standard Deviation					0.0326

Note: M_{ut} = Tested moment capacities
M_{uen} = Moment capacity based on effective net section

TABLE 7-2
COMPARISON OF TEST RESULTS
(Based on Effective Net Section Approach)
UMR TEST SEQUENCE No. 2

Beam Specimen No.	h/t	a/h	M_{ut} (k-in)	M_{uen} (k-in)	$(M_{ut})/(M_{uen})$
2,16,1&2(H)	34	0.74	29.17	26.87	1.086
2,16,3&4(H)	35	0.74	29.47	27.30	1.079
2,20,1&2(H)	62	0.73	14.65	13.52	1.084
2,20,3&4(H)	62	0.73	15.33	13.50	1.136
Mean					1.096
Standard Deviation					0.0267
3,14,1&2(H)	45	0.47	86.99	86.42	1.007
3,14,3&4(H)	45	0.47	85.68	82.41	1.040
3,18,1&2(H)	73	0.47	34.15	31.88	1.071
3,18,3&4(H)	73	0.47	32.39	31.33	1.034
3,20,1&2(H)	90	0.47	26.35	27.64	0.953
3,20,3&4(H)	90	0.47	24.40	27.68	(0.882)
3,20,5&6(H)	90	0.47	28.88	27.52	1.049
Mean					1.026
Mean					(1.005)*
Standard Deviation					0.0412
Standard Deviation					(0.0661)*

See Table 7-1 for Notes

* Includes Beam Specimen No. 3,20,3&4(H)

Table 8
COMPARISON OF THE TESTED TO COMPUTED MOMENT CAPACITIES
UMR TEST SEQUENCES NO. 1 & 2

	M(tested)/M(computed)					
	y/h=0.36		y/h=0.47		y/h=0.74	
	MEAN	STD	MEAN	STD	MEAN	STD
1986 AISI	0.995	0.0495	0.909	0.0475	0.924	0.0619
Method I	1.124	0.2154	0.956	0.0524	0.974	0.0666
Method II	1.021	0.0423	0.939	0.0528	1.093	0.0291
Method III	1.031	0.0367	0.984	0.0558	1.096	0.0267

Note:

Method I: Based on Modified Effective Area (b_2=0)
Method II: Based on Net Section Approach
Method III: Based on Effective Net Section Approach

TABLE 9-1
COMPARISON OF TEST RESULTS
(Based on Model A)
UMR TEST SEQUENCE No. 1

Beam Specimen No.	(1) M_{ut}	(2) $M_{uc,d}$	(3) $M_{uc,d}$	(4) $M_{uc,d}$	(1)/(2)	(1)/(3)	(1)/(4)
12,14,1&2(H)	219.52	290.30	291.43	295.53	0.756	0.753	0.743
12,14,3&4(H)	229.87	289.21	290.41	294.57	0.795	0.792	0.780
12,16,1&2(H)	135.97	137.35	139.72	147.15	0.990	0.973	0.924
12,16,3&4(H)	148.27	130.22	132.45	139.57	1.139	1.119	1.062
Mean					0.920	0.909	0.877
Standard Deviation					0.1783	0.1695	0.1458

Notes: 1. Method I- $M_{uc,d} = F_d \, S_{ex,Fy}$

2. The section modulus is the effective section modulus utilized the yielding stress.

3. (1)M_{ut}: the test results
(2)$M_{uc,d}$: the computed moment based on Eq. 8a
(3)$M_{uc,d}$: the computed moment based on Eq. 8b
(4)$M_{uc,d}$: the computed moment based on Eq. 8c
(1)/(2): the ratio of $M_{ut}/M_{uc,d}$

TABLE 9-2
COMPARISON OF TEST RESULTS
(Based on Model A)
UMR TEST SEQUENCE No. 2

Beam Specimen No.	(1) M_{ut}	(2) $M_{uc,d}$	(3) $M_{uc,d}$	(4) $M_{uc,d}$	(1)/(2)	(1)/(3)	(1)/(4)
6A,18,1&2(H)	53.58	49.51	50.92	53.49	1.082	1.052	1.002
6A,18,3&4(H)	55.38	49.63	51.05	53.61	1.116	1.085	1.033
6,20,1&2(H)	38.88	25.08	26.07	27.90	1.550	1.491	1.394
Mean					1.099	1.069	1.018
8,18,1&2(H)	87.18	59.60	62.98	70.50	1.463	1.384	1.237
Mean					1.463	1.384	1.237
12,16,1&2(H)	198.93	172.68	176.33	187.82	1.152	1.128	1.059
12,16,3&4(H)	197.52	167.88	171.37	182.58	1.177	1.153	1.082
12,16,5&6(H)	195.93	169.49	173.02	184.36	1.156	1.132	1.063
12,16,7&8(H)	204.33	168.88	172.40	183.59	1.210	1.185	1.113
12,16,1&2(N)	199.38	180.66	184.23	195.81	1.104	1.082	1.018
12,16,3&4(N)	207.03	179.43	182.99	194.56	1.154	1.131	1.064
Mean					1.159	1.135	1.067
Standard Deviation					0.0347	0.0338	0.0311

See Table 9-1 for Notes

TABLE 9-3
COMPARISON OF TEST RESULTS
(Based on Model A)
SCHUSTER TEST SEQUENCE No. 3

Beam Specimen No.	(1) M_{ut}	(2) $M_{uc,d}$	(3) $M_{uc,d}$	(4) $M_{uc,d}$	(1)/(2)	(1)/(3)	(1)/(4)
BS1	74.88	68.42	69.81	72.99	1.094	1.073	1.026
BS2	76.21	68.42	69.81	72.99	1.114	1.092	1.044
BP4-40	75.85	67.14	68.52	71.63	1.130	1.107	1.059
BP5-40	73.64	67.14	68.52	71.63	1.097	1.075	1.028
BP6-40	76.21	67.14	68.52	71.63	1.135	1.112	1.064
BP7-65	75.23	67.75	69.07	72.08	1.110	1.089	1.044
BP8-65	76.38	67.08	68.46	71.57	1.139	1.116	1.067
BP9-65	76.21	67.14	68.52	71.63	1.135	1.112	1.064
CS1	80.10	76.29	78.22	82.42	1.050	1.024	0.972
CS2	80.10	76.29	78.22	82.42	1.050	1.024	0.972
CS3	82.22	75.79	77.75	82.03	1.085	1.057	1.002
CP4-40	82.84	74.57	76.54	80.83	1.111	1.082	1.025
CP5-40	78.68	74.57	76.54	80.83	1.055	1.028	0.973
CP6-40	83.37	73.57	75.57	79.91	1.133	1.103	1.043
CP7-65	81.69	72.85	74.89	79.26	1.121	1.091	1.031
CP8-65	81.78	74.51	76.48	80.78	1.098	1.069	1.012
CP9-65	81.87	72.85	74.89	79.26	1.124	1.093	1.033
Mean					1.105	1.079	1.027
Standard Deviation					0.0299	0.0304	0.0317

See Table 9-1 for Notes

TABLE 9-4
COMPARISON OF TEST TO COMPUTED MOMENT CAPACITIES
(Based on Tables 9-1, 9-2 and 9-3)

	M(tested)/M(computed)					
	(1)		(2)		(3)	
	MEAN	STD	MEAN	STD	MEAN	STD
UMR Test Sequence No. 1	0.920	0.1783	0.909	0.1695	0.877	0.1458
UMR Test Sequence No. 2	1.144	0.0414	1.119	0.0430	1.054	0.0357
SCHUSTER Test Sequence No. 3	1.105	0.0299	1.079	0.0304	1.027	0.0317
Combined All Three Sequences	1.090	0.0971	1.067	0.0920	1.014	0.0800

Notes: 1. Method I- $M_{uc,d} = F_d \, S_{ex,Fy}$

2. (1): the computed moment based on Eq. 8a
(2): the computed moment based on Eq. 8b
(3): the computed moment based on Eq. 8c

TABLE 10-1
COMPARISON OF TEST RESULTS
(Based on Model A)
UMR TEST SEQUENCE No. 1

Beam Specimen No.	(1) M_{ut}	(2) $M_{uc,d}$	(3) $M_{uc,d}$	(4) $M_{uc,d}$	(1)/(2)	(1)/(3)	(1)/(4)
12,14,1&2(H)	219.52	288.59	290.08	295.21	0.761	0.757	0.734
12,14,3&4(H)	229.87	288.88	290.36	295.20	0.796	0.792	0.779
12,16,1&2(H)	135.97	159.17	162.54	173.62	0.854	0.837	0.783
12,16,3&4(H)	148.27	154.96	157.93	169.11	0.957	0.939	0.877
Mean					0.842	0.831	0.793
Standard Deviation					0.0857	0.0789	0.0601

Notes: 1. Method II- $M_{uc,d} = F_d \; S_{ex,d}$

2. The section modulus is the effective section modulus based on the Eqs. 9a, 9b and 9c.

3. See Table 9-1 for Notes

TABLE 10-2
COMPARISON OF TEST RESULTS
(Based on Model A)
UMR TEST SEQUENCE No. 2

Beam Specimen No.	(1) M_{ut}	(2) $M_{uc,d}$	(3) $M_{uc,d}$	(4) $M_{uc,d}$	(1)/(2)	(1)/(3)	(1)/(4)
6A,18,1&2(H)	53.58	45.95	47.84	51.52	1.166	1.120	1.040
6A,18,3&4(H)	55.38	46.03	47.93	51.60	1.203	1.156	1.073
6,20,1&2(H)	38.88	32.66	34.99	39.45	1.190	1.111	0.986
Mean					1.186	1.129	1.033
8,18,1&2(H)	87.18	70.81	75.40	86.10	1.231	1.156	1.013
Mean					1.231	1.156	1.013
12,16,1&2(H)	198.93	203.88	209.08	225.82	0.976	0.951	0.881
12,16,3&4(H)	197.52	200.04	204.91	221.76	0.987	0.964	0.891
12,16,5&6(H)	195.93	201.55	206.54	223.25	0.972	0.949	0.878
12,16,7&8(H)	204.33	202.93	208.00	224.71	1.007	0.982	0.909
12,16,1&2(N)	199.38	216.37	221.57	238.70	0.921	0.900	0.835
12,16,3&4(N)	207.03	214.72	219.79	237.00	0.964	0.942	0.874
Mean					0.971	0.948	0.878
Standard Deviation					0.0287	0.0274	0.0245

See Table 10-1 for Notes

TABLE 10-3
COMPARISON OF TEST RESULTS
(Based on Model A)
SCHUSTER TEST SEQUENCE No. 3

Beam Specimen No.	(1) M_{ut}	(2) $M_{uc,d}$	(3) $M_{uc,d}$	(4) $M_{uc,d}$	(1)/(2)	(1)/(3)	(1)/(4)
BS1	74.88	64.13	65.98	70.40	1.168	1.135	1.064
BS2	76.21	64.13	65.98	70.40	1.188	1.155	1.083
BP4-40	75.85	62.97	64.79	69.14	1.205	1.171	1.097
BP5-40	73.64	62.97	64.79	69.14	1.169	1.137	1.065
BP6-40	76.21	62.97	64.79	69.14	1.210	1.176	1.102
BP7-65	75.23	63.16	64.91	69.10	1.191	1.159	1.089
BP8-65	76.38	62.97	64.79	69.14	1.213	1.179	1.105
BP9-65	76.21	62.97	64.79	69.14	1.210	1.176	1.102
CS1	80.10	74.10	76.64	82.47	1.081	1.045	0.971
CS2	80.10	74.10	76.64	82.47	1.081	1.045	0.971
CS3	82.22	73.99	76.65	82.70	1.111	1.073	0.994
CP4-40	82.84	73.84	76.47	82.48	1.122	1.083	1.004
CP5-40	78.68	73.84	76.47	82.48	1.066	1.029	0.954
CP6-40	83.37	73.69	76.43	82.67	1.131	1.091	1.008
CP7-65	81.69	73.44	76.18	82.39	1.112	1.072	0.992
CP8-65	81.78	74.32	76.95	83.00	1.100	1.063	0.985
CP9-65	81.87	73.44	76.18	82.39	1.115	1.075	0.994
Mean					1.145	1.110	1.034
Standard Deviation					0.0513	0.0532	0.0552

See Table 10-1 for Notes

TABLE 10-4
COMPARISON OF TEST TO COMPUTED MOMENT CAPACITIES
(Based on Tables 10-1, 10-2 and 10-3)

	M(tested)/M(computed)					
	(1)		(2)		(3)	
	MEAN	STD	MEAN	STD	MEAN	STD
UMR Test Sequence No. 1	0.842	0.0857	0.831	0.0789	0.793	0.0601
UMR Test Sequence No. 2	1.062	0.1198	1.023	0.1000	0.938	0.0824
SCHUSTER Test Sequence No. 3	1.145	0.0513	1.110	0.0532	1.034	0.0552
Combined All Three Sequences	1.079	0.1286	1.046	0.1173	0.972	0.1042

Notes: 1. Method II- $M_{uc,d} = F_d \, S_{ex,d}$

2. See Table 9-4 for Notes

TABLE 11-1
COMPARISON OF TEST RESULTS
(Based on Model A)
UMR TEST SEQUENCE No. 1

Beam Specimen No.	(1) M_{ut}	(2) $M_{uc,d}$	(3) $M_{uc,d}$	(4) $M_{uc,d}$	(1)/(2)	(1)/(3)	(1)/(4)
12,14,1&2(H)	219.52	274.67	274.40	272.90	0.799	0.800	0.804
12,14,3&4(H)	229.87	273.42	273.14	271.62	0.841	0.842	0.846
12,16,1&2(H)	135.97	138.80	140.92	147.74	0.980	0.965	0.920
12,16,3&4(H)	148.27	133.66	135.55	142.47	1.109	1.094	1.041
Mean					0.932	0.925	0.903
Standard Deviation					0.1410	0.1325	0.1039

Notes: 1. Method III- $M_{uc,d} = F_d \ S_{ex,Fd}$

2. The section modulus is the effective section modulus by using the AISI Specification Eqs. which represents the local buckling mode, the local buckling stress is replaced by distortional buckling stress for the web and using the Eqs. 9a, 9b and 9c which illustrates the distortional buckling mode for the flange.

3. See Table 9-1 for Notes

TABLE 11-2
COMPARISON OF TEST RESULTS
(Based on Model A)
UMR TEST SEQUENCE No. 2

Beam Specimen No.	(1) M_{ut}	(2) $M_{uc,d}$	(3) $M_{uc,d}$	(4) $M_{uc,d}$	(1)/(2)	(1)/(3)	(1)/(4)
6A,18,1&2(H)	53.58	46.82	48.66	52.22	1.144	1.101	1.026
6A,18,3&4(H)	55.38	46.91	48.75	52.30	1.181	1.136	1.059
6,20,1&2(H)	38.88	32.28	33.51	35.83	1.204	1.160	1.085
Mean					1.176	1.132	1.057
8,18,1&2(H)	87.18	68.92	72.65	81.04	1.265	1.200	1.076
Mean					1.265	1.200	1.076
12,16,1&2(H)	198.93	181.07	184.53	195.41	1.099	1.078	1.018
12,16,3&4(H)	197.52	176.81	180.06	191.05	1.117	1.097	1.034
12,16,5&6(H)	195.93	178.60	181.92	192.78	1.097	1.077	1.016
12,16,7&8(H)	204.33	179.88	183.25	194.10	1.136	1.115	1.053
12,16,1&2(N)	199.38	193.03	196.45	207.43	1.033	1.015	0.961
12,16,3&4(N)	207.03	191.09	194.42	205.49	1.083	1.065	1.007
Mean					1.094	1.075	1.015
Standard Deviation					0.0351	0.0340	0.0310

See Table 11-1 for Notes

TABLE 11-3
COMPARISON OF TEST RESULTS
(Based on Model A)
SCHUSTER TEST SEQUENCE No. 3

Beam Specimen No.	(1) M_{ut}	(2) $M_{uc,d}$	(3) $M_{uc,d}$	(4) $M_{uc,d}$	(1)/(2)	(1)/(3)	(1)/(4)
BS1	74.88	63.06	64.24	67.02	1.187	1.166	1.117
BS2	76.21	63.06	64.24	67.02	1.209	1.186	1.137
BP4-40	75.85	61.84	63.02	65.75	1.227	1.204	1.154
BP5-40	73.64	61.84	63.02	65.75	1.191	1.169	1.120
BP6-40	76.21	61.84	63.02	65.75	1.232	1.209	1.159
BP7-65	75.23	61.74	62.84	65.43	1.218	1.197	1.150
BP8-65	76.38	61.84	63.02	65.75	1.235	1.212	1.162
BP9-65	76.21	61.84	63.02	65.75	1.232	1.209	1.159
CS1	80.10	72.35	74.07	77.94	1.107	1.081	1.028
CS2	80.10	72.35	74.07	77.94	1.107	1.081	1.028
CS3	82.22	72.62	74.44	78.52	1.132	1.105	1.047
CP4-40	82.84	72.00	73.80	77.85	1.151	1.122	1.064
CP5-40	78.68	72.00	73.80	77.85	1.093	1.066	1.011
CP6-40	83.37	72.22	74.14	78.40	1.154	1.124	1.063
CP7-65	81.69	71.91	73.83	78.08	1.136	1.106	1.046
CP8-65	81.78	72.35	74.16	78.24	1.130	1.103	1.045
CP9-65	81.87	71.91	73.83	78.08	1.139	1.109	1.049
Mean					1.169	1.144	1.091
Standard Deviation					0.0481	0.0519	0.0554

See Table 11-1 for Notes

TABLE 11-4
COMPARISON OF TEST TO COMPUTED MOMENT CAPACITIES
(Based on Tables 11-1, 11-2 and 11-3)

	M(tested)/M(computed)					
	(1)		(2)		(3)	
	MEAN	STD	MEAN	STD	MEAN	STD
UMR Test Sequence No. 1	0.932	0.1410	0.925	0.1325	0.903	0.1039
UMR Test Sequence No. 2	1.136	0.0667	1.104	0.0521	1.034	0.0366
SCHUSTER Test Sequence No. 3	1.169	0.0481	1.144	0.0519	1.091	0.0554
Combined All Three Sequences	1.121	0.1028	1.098	0.0967	1.046	0.0863

Notes: 1. Method III- $M_{uc,d} = F_d S_{ex,Fd}$

2. See Table 9-4 for Notes

TABLE 12-1
COMPARISON OF TEST RESULTS
(Based on Model A)
UMR TEST SEQUENCE No. 1

Beam Specimen No.	(1) M_{ut}	(2) $M_{uc,d}$	(3) $M_{uc,d}$	(4) $M_{uc,d}$	(1)/(2)	(1)/(3)	(1)/(4)
12,14,1&2(H)	219.52	290.31	291.39	295.51	0.756	0.753	0.743
12,14,3&4(H)	229.87	289.21	290.38	294.59	0.795	0.792	0.780
12,16,1&2(H)	135.97	151.13	152.54	158.37	0.900	0.891	0.859
12,16,3&4(H)	148.27	147.73	148.55	152.79	1.004	0.998	0.970
Mean					0.864	0.859	0.838
Standard Deviation					0.1115	0.1096	0.1004

Notes: 1. Method IV- $M_{uc,d} = F_d S_{ex,dy}$

2. The section modulus is the effective section modulus based on the elastic or inelastic distortional buckling stress.

3. (1)M_{ut}: the test results
(2)$M_{uc,d}$: the computed moment based on Eq. 8a
(3)$M_{uc,d}$: the computed moment based on Eq. 8b
(4)$M_{uc,d}$: the computed moment based on Eq. 8c
(1)/(2): the ratio of $M_{ut}/M_{uc,d}$

TABLE 12-2
COMPARISON OF TEST RESULTS
(Based on Model A)
UMR TEST SEQUENCE No. 2

Beam Specimen No.	(1) M_{ut}	(2) $M_{uc,d}$	(3) $M_{uc,d}$	(4) $M_{uc,d}$	(1)/(2)	(1)/(3)	(1)/(4)
6A,18,1&2(H)	53.58	52.13	53.47	55.80	1.028	1.002	0.960
6A,18,3&4(H)	55.38	52.19	53.60	55.92	1.061	1.033	0.990
6,20,1&2(H)	38.88	33.77	35.52	36.88	1.151	1.095	1.054
Mean					1.080	1.043	1.001
8,18,1&2(H)	87.18	80.18	83.04	87.82	1.087	1.050	0.993
Mean					1.087	1.050	0.993
12,16,1&2(H)	198.93	196.83	199.70	208.87	1.011	0.996	0.952
12,16,3&4(H)	197.52	194.61	197.06	210.28	1.015	1.002	0.939
12,16,5&6(H)	195.93	195.43	198.16	207.33	1.003	0.989	0.945
12,16,7&8(H)	204.33	195.10	198.00	205.75	1.047	1.032	0.993
12,16,1&2(N)	199.38	208.80	211.71	219.31	0.955	0.942	0.909
12,16,3&4(N)	207.03	207.61	209.52	215.83	0.997	0.988	0.959
Mean					1.005	0.992	0.950
Standard Deviation					0.0299	0.0291	0.0274

See Table 12-1 for Notes

TABLE 12-3
COMPARISON OF TEST RESULTS
(Based on Model A)
SCHUSTER TEST SEQUENCE No. 3

Beam Specimen No.	(1) M_{ut}	(2) $M_{uc,d}$	(3) $M_{uc,d}$	(4) $M_{uc,d}$	(1)/(2)	(1)/(3)	(1)/(4)
BS1	74.88	70.90	72.36	75.64	1.056	1.035	0.990
BS2	76.21	70.90	72.36	75.64	1.075	1.053	1.008
BP4-40	75.85	69.65	71.08	74.31	1.089	1.067	1.021
BP5-40	73.64	69.65	71.08	74.31	1.057	1.036	0.991
BP6-40	76.21	69.65	71.08	74.31	1.094	1.072	1.026
BP7-65	75.23	69.48	70.82	73.92	1.083	1.062	1.018
BP8-65	76.38	68.77	70.18	73.38	1.111	1.088	1.041
BP9-65	76.21	69.65	71.08	74.31	1.094	1.072	1.026
CS1	80.10	83.20	85.29	89.89	0.963	0.939	0.891
CS2	80.10	83.20	85.29	89.89	0.963	0.939	0.891
CS3	82.22	82.64	84.79	89.46	0.995	0.970	0.919
CP4-40	82.84	83.27	85.49	90.27	0.995	0.969	0.918
CP5-40	78.68	83.27	85.49	90.27	0.945	0.920	0.872
CP6-40	83.37	83.52	85.82	90.67	0.998	0.971	0.920
CP7-65	81.69	83.32	85.64	90.65	0.980	0.954	0.901
CP8-65	81.78	83.22	85.42	90.22	0.983	0.957	0.906
CP9-65	81.87	83.32	85.64	90.65	0.983	0.956	0.903
Mean					1.027	1.004	0.955
Standard Deviation					0.0564	0.0581	0.0603

See Table 12-1 for Notes

TABLE 12-4
COMPARISON OF TEST TO COMPUTED MOMENT CAPACITIES
(Based on Tables 12-1, 12-2 and 12-3)

	M(tested)/M(computed)					
	(1)		(2)		(3)	
	MEAN	STD	MEAN	STD	MEAN	STD
UMR Test Sequence No. 1	0.864	0.1115	0.859	0.1096	0.838	0.1004
UMR Test Sequence No. 2	1.023	0.0388	1.004	0.0319	0.960	0.0283
SCHUSTER Test Sequence No. 3	1.027	0.0564	1.004	0.0581	0.955	0.0603
Combined All Three Sequences	1.009	0.0841	0.988	0.0781	0.945	0.0722

Notes: 1. Method IV- $M_{uc,d} = F_d \, S_{ex,dy}$

2. (1): the computed moment based on Eq. 8a
   (2): the computed moment based on Eq. 8b
   (3): the computed moment based on Eq. 8c

TABLE 13-1
COMPARISON OF TEST RESULTS
(Based on Model B)
UMR TEST SEQUENCE No. 1

Beam Specimen No.	M_{ut}	$M_{uc,d}$	$M_{ut}/M_{uc,d}$
12,14,1&2(H)	219.52	215.74	1.018
12,14,3&4(H)	229.87	217.18	1.058
12,16,1&2(H)	135.97	21.19	6.417
12,16,3&4(H)	148.27	19.56	7.580
Mean			4.018
Standard Deviation			3.4739

Note: Method V- $M_{uc,d} = F_n S_e$

TABLE 13-2
COMPARISON OF TEST RESULTS
(Based on Model B)
UMR TEST SEQUENCE No. 2

Beam Specimen No.	M_{ut}	$M_{uc,d}$	$M_{ut}/M_{uc,d}$
6A,18,1&2(H)	53.58	42.04	1.275
6A,18,3&4(H)	55.38	42.27	1.310
6,20,1&2(H)	38.88	6.18	6.291
Mean			2.959
8,18,1&2(H)	87.18	14.11	6.177
Mean			
12,16,1&2(H)	198.93	25.26	7.875
12,16,3&4(H)	197.52	24.17	8.174
12,16,5&6(H)	195.93	24.46	8.009
12,16,7&8(H)	204.33	24.34	8.395
12,16,1&2(N)	199.38	26.70	7.468
12,16,3&4(N)	207.03	26.50	7.813
Mean			7.956
Standard Deviation			0.3188

TABLE 13-3
COMPARISON OF TEST RESULTS
(Based on Model B)
SCHUSTER TEST SEQUENCE No. 3

Beam Specimen No.	M_{ut}	$M_{uc,d}$	$M_{ut}/M_{uc,d}$
BS1	74.88	31.02	2.414
BS2	76.21	31.02	2.457
BP4-40	75.85	30.25	2.507
BP4-50	73.64	30.25	2.434
BP4-60	76.21	30.25	2.519
BP7-65	75.23	30.07	2.502
BP8-65	76.38	29.97	2.549
BP9-65	76.21	30.25	2.519
CS1	80.10	26.90	2.977
CS2	80.10	26.90	2.977
CS3	82.22	26.91	3.055
CP4-40	82.84	25.39	3.262
CP5-40	78.68	25.39	3.098
CP6-40	83.37	25.10	3.322
CP7-65	81.69	25.33	3.225
CP8-65	81.78	25.46	3.212
CP9-65	81.87	25.33	3.232
Mean			2.839
Standard Deviation			0.3544

TABLE 14-1
COMPARISON OF TEST RESULTS
(Based on the Flat Widths of Flange and Web)
UMR TEST SEQUENCE No. 1

Beam Specimen No.	(1) M_{ut}	(2) $M_{uc,d}$	(3) $M_{uc,d}$	(4) $M_{uc,d}$	(1)/(2)	(1)/(3)	(1)/(4)
12,14,1&2(H)	219.52	322.95	224.60	322.95	0.680	0.977	0.680
12,14,3&4(H)	229.87	322.29	208.30	322.29	0.713	1.104	0.713
12,16,1&2(H)	135.97	239.11	144.05	196.28	0.569	0.944	0.693
12,16,3&4(H)	148.27	221.23	133.88	183.17	0.670	1.107	0.809
Mean					0.658	1.033	0.724
Standard Deviation					0.0621	0.0848	0.0584

Notes: 1. Method VI- $M_{uc,d} = F_y S_{ex,Fk}$

2. The section modulus is the effective section modulus employed the elastic or inelastic distortional buckling stress.

3. (1)M_{ut}: the test results
(2)$M_{uc,d}$:the computed moment based on Eq. 15a
(3)$M_{uc,d}$:the computed moment based on Eq. 15b
(4)$M_{uc,d}$:the computed moment based on Eq. 15c
(1)/(2): the ratio of $M_{ut}/M_{uc,d}$

TABLE 14-2
COMPARISON OF TEST RESULTS
(Based on the Flat Widths of Flange and Web)
UMR TEST SEQUENCE No. 2

Beam Specimen No.	(1) M_{ut}	(2) $M_{uc,d}$	(3) $M_{uc,d}$	(4) $M_{uc,d}$	(1)/(2)	(1)/(3)	(1)/(4)
6A,18,1&2(H)	53.58	67.37	55.04	67.20	0.795	0.974	0.797
6A,18,3&4(H)	55.38	67.52	54.22	67.52	0.820	1.021	0.820
6,20,1&2(H)	38.88	67.97	68.74	63.20	0.572	0.566	0.615
Mean					0.808	0.998	0.809
8,18,1&2(H)	87.18	137.56	94.73	121.53	0.634	0.920	0.717
Mean					0.634	0.920	0.717
12,16,1&2(H)	198.93	325.53	197.60	263.61	0.611	1.007	0.755
12,16,3&4(H)	197.52	310.79	192.53	255.43	0.636	1.026	0.773
12,16,5&6(H)	195.93	317.52	194.00	258.43	0.617	1.010	0.758
12,16,7&8(H)	204.33	321.13	195.61	260.65	0.636	1.045	0.784
12,16,1&2(N)	199.38	340.87	208.11	279.15	0.585	0.958	0.714
12,16,3&4(N)	207.03	337.97	205.30	274.41	0.613	1.008	0.754
Mean					0.616	1.009	0.756
Standard Deviation					0.0189	0.0290	0.0239

See Table 14-1 for Notes

TABLE 14-3
COMPARISON OF TEST RESULTS
(Based on the Flat Widths of Flange and Web)
SCHUSTER TEST SEQUENCE No. 3

Beam Specimen No.	(1) M_{ut}	(2) $M_{uc,d}$	(3) $M_{uc,d}$	(4) $M_{uc,d}$	(1)/(2)	(1)/(3)	(1)/(4)
BS1	74.88	92.16	74.45	89.71	0.812	1.006	0.835
BS2	76.21	92.16	74.45	89.71	0.827	1.024	0.849
BP4-40	75.85	90.54	73.30	88.03	0.838	1.035	0.862
BP5-40	73.64	90.54	73.30	88.03	0.813	1.005	0.837
BP6-40	76.21	90.54	73.30	88.03	0.842	1.040	0.866
BP7-65	75.23	90.13	68.08	88.43	0.835	1.105	0.851
BP8-65	76.38	90.54	73.30	88.03	0.844	1.042	0.868
BP9-65	76.21	90.54	73.30	88.03	0.842	1.040	0.866
CS1	80.10	112.70	82.62	105.41	0.711	0.970	0.760
CS2	80.10	112.70	82.62	105.41	0.711	0.970	0.760
CS3	82.22	112.74	87.12	104.40	0.729	0.944	0.788
CP4-40	82.84	113.11	82.50	104.04	0.732	1.004	0.796
CP5-40	78.68	113.11	82.50	104.04	0.696	0.954	0.756
CP6-40	83.37	113.16	86.91	103.07	0.737	0.959	0.809
CP7-65	81.69	112.68	87.51	101.97	0.725	0.934	0.801
CP8-65	81.78	113.91	81.79	104.58	0.718	1.000	0.782
CP9-65	81.87	112.68	87.51	101.97	0.727	0.936	0.803
Mean					0.773	0.998	0.817
Standard Deviation					0.0584	0.0468	0.0400

See Table 14-1 for Notes

TABLE 14-4
COMPARISON OF TEST TO COMPUTED MOMENT CAPACITIES
(Based on Tables 14-1, 14-2 and 14-3)

	M(tested)/M(computed)					
	(1)		(2)		(3)	
	MEAN	STD	MEAN	STD	MEAN	STD
UMR Test Sequence No. 1	0.658	0.0621	1.033	0.0848	0.724	0.0584
UMR Test Sequence No. 2	0.652	0.0849	1.006	0.0280	0.764	0.0347
SCHUSTER Test Sequence No. 3	0.773	0.0584	0.998	0.0468	0.817	0.0400
Combined All Three Sequences	0.719	0.0895	1.005	0.0486	0.789	0.0531

Notes: 1. Method VI- $M_{uc,d} = F_y \; S_{ex,Fk}$

2. (1): the computed moment based on Eq. 15a
   (2): the computed moment based on Eq. 15b
   (3): the computed moment based on Eq. 15c

TABLE 15-1
COMPARISON OF TEST RESULTS
UMR TEST SEQUENCE No. 1

Beam Specimen No.	(1) M_{ut}	(2) $M_{uc,d}$	(3) $M_{uc,d}$	(1)/(2)	(1)/(3)
12,14,1&2(H)	219.52	291.43	292.08	0.753	0.752
12,14,3&4(H)	229.87	290.41	290.28	0.792	0.792
12,16,1&2(H)	135.97	139.72	131.29	0.973	1.036
12,16,3&4(H)	148.27	132.45	124.70	1.119	1.189
Mean				0.909	0.942
Standard Deviation				0.1695	0.2069

Notes: 1. Method VII- $M_{uc,d} = F_{d,p}\ S_{ex,p}$

2. (1): M_{ut}: the test results
(2): See Table 9-1
(3): $M_{uc,d}$: the computed based on Eq. 18
(1)/(2): the ratio of $M_{ut}/M_{uc,d}$

TABLE 15-2
COMPARISON OF TEST RESULTS
UMR TEST SEQUENCE No. 2

Beam Specimen No.	(1) M_{ut}	(2) $M_{uc,d}$	(3) $M_{uc,d}$	(1)/(2)	(1)/(3)
6A,18,1&2(H)	53.58	50.92	53.08	1.052	1.009
6A,18,3&4(H)	55.38	51.05	53.16	1.085	1.042
6,20,1&2(H)	38.88	26.07	27.75	1.491	1.401
MEAN				1.069	1.026
8,18,1&2(H)	87.18	62.98	62.28	1.384	1.400
MEAN				1.384	1.400
12,16,1&2(H)	198.93	176.33	172.02	1.128	1.156
12,16,3&4(H)	197.52	171.37	167.96	1.153	1.176
12,16,5&6(H)	195.93	173.02	169.96	1.132	1.153
12,16,7&8(H)	204.33	172.40	168.25	1.185	1.214
12,16,1&2(N)	199.38	184.23	184.58	1.082	1.080
12,16,3&4(N)	207.03	182.99	183.38	1.131	1.129
Mean				1.135	1.151
Standard Deviation				0.0338	0.0450

See Table 15-1 for Notes

TABLE 15-3
COMPARISON OF TEST RESULTS
SCHUSTER TEST SEQUENCE No. 3

Beam Specimen No.	(1) M_{ut}	(2) $M_{uc,d}$	(3) $M_{uc,d}$	(1)/(2)	(1)/(3)
BS1	74.88	69.81	70.40	1.073	1.064
BS2	76.21	69.81	70.40	1.092	1.082
BP4-40	75.85	68.52	68.95	1.107	1.100
BP5-40	73.64	68.52	68.95	1.075	1.068
BP6-40	76.21	68.52	68.95	1.112	1.105
BP7-65	75.23	69.07	69.27	1.089	1.086
BP8-65	76.38	68.46	68.89	1.116	1.109
BP9-65	76.21	68.52	68.95	1.112	1.105
CS1	80.10	78.22	77.31	1.024	1.036
CS2	80.10	78.22	77.31	1.024	1.036
CS3	82.22	77.75	76.89	1.057	1.069
CP4-40	82.84	76.54	75.40	1.082	1.099
CP5-40	78.68	76.54	75.40	1.028	1.044
CP6-40	83.37	75.57	74.48	1.103	1.119
CP7-65	81.69	74.89	74.01	1.091	1.104
CP8-65	81.78	76.48	75.26	1.069	1.087
CP9-65	81.87	74.89	74.01	1.093	1.106
Mean				1.079	1.083
Standard Deviation				0.0304	0.0265

See Table 15-1 for Notes

TABLE 15-4
COMPARISON OF TEST TO COMPUTED MOMENT CAPACITIES
(Based on Tables 15-1, 15-2 and 15-3)

	M(tested)/M(computed)			
	(1)		(2)	
	MEAN	STD	MEAN	STD
UMR Test Sequence No. 1	0.909	0.1695	0.942	0.2069
UMR Test Sequence No. 2	1.119	0.0430	1.120	0.0701
SCHUSTER Test Sequence No. 3	1.079	0.0304	1.083	0.0265
Combined All Three Sequences	1.067	0.0920	1.074	0.0967

Notes: 1. Method VII- $M_{uc,d} = F_{d,p} S_{ex,p}$

2. (1): See Table 9-4
(2): the computed moment based on Eq. 18

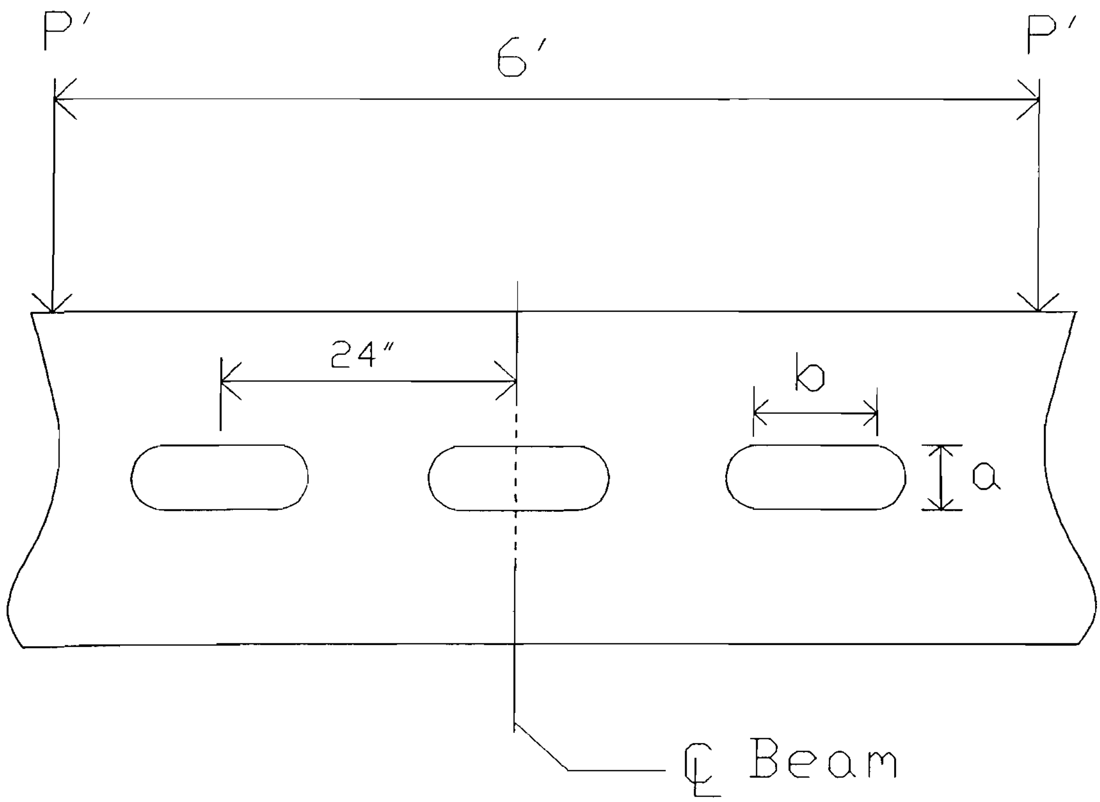

Figure 1. Opening Configuration

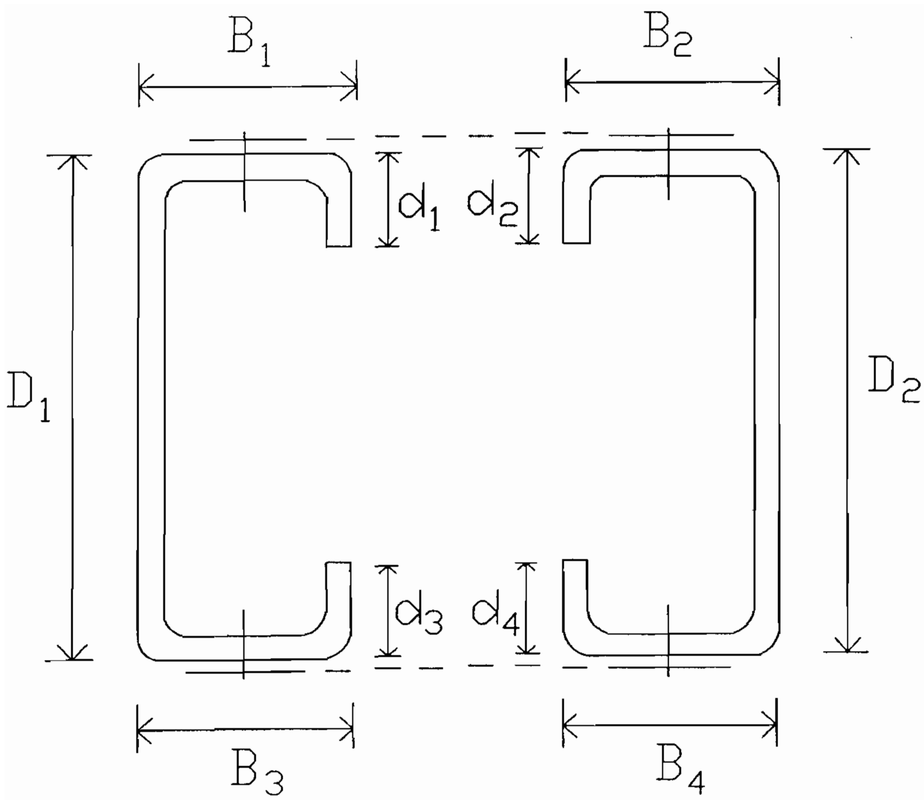

Figure 2. Beam Cross-Section

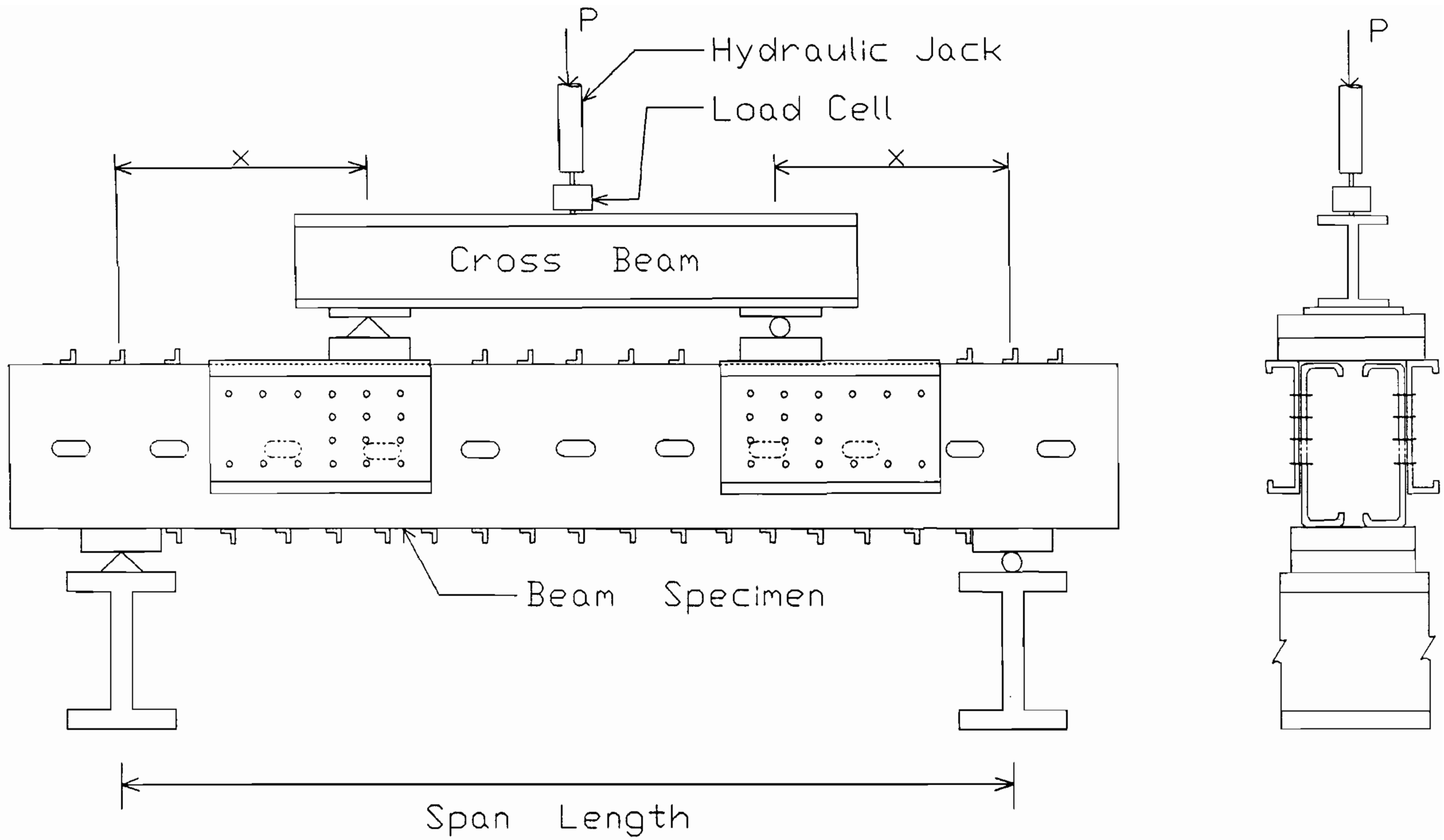

Figure 3. Test Setup

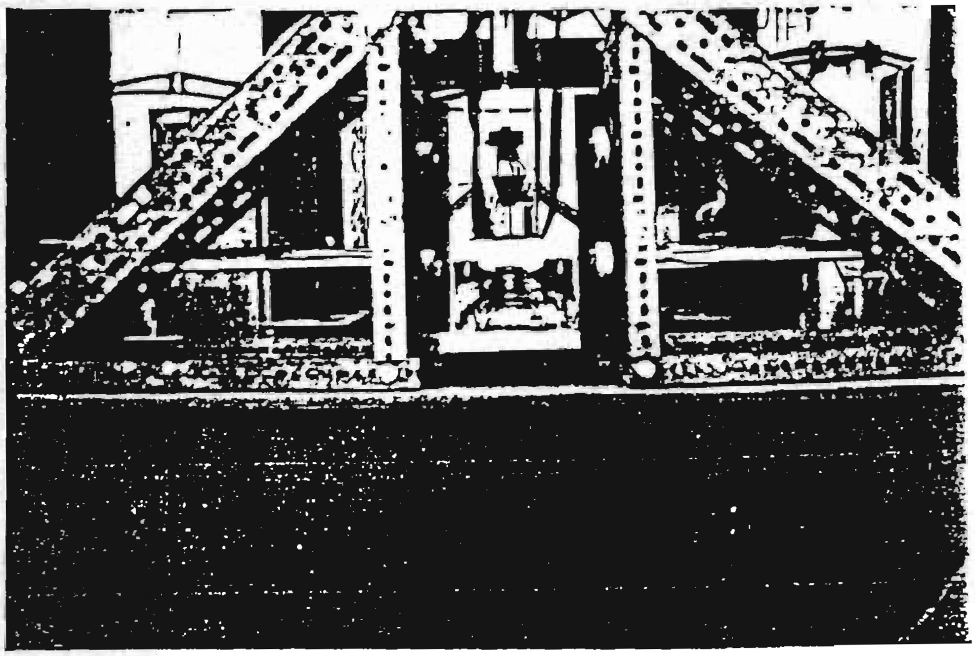

Figure 4. Support at End of Beam

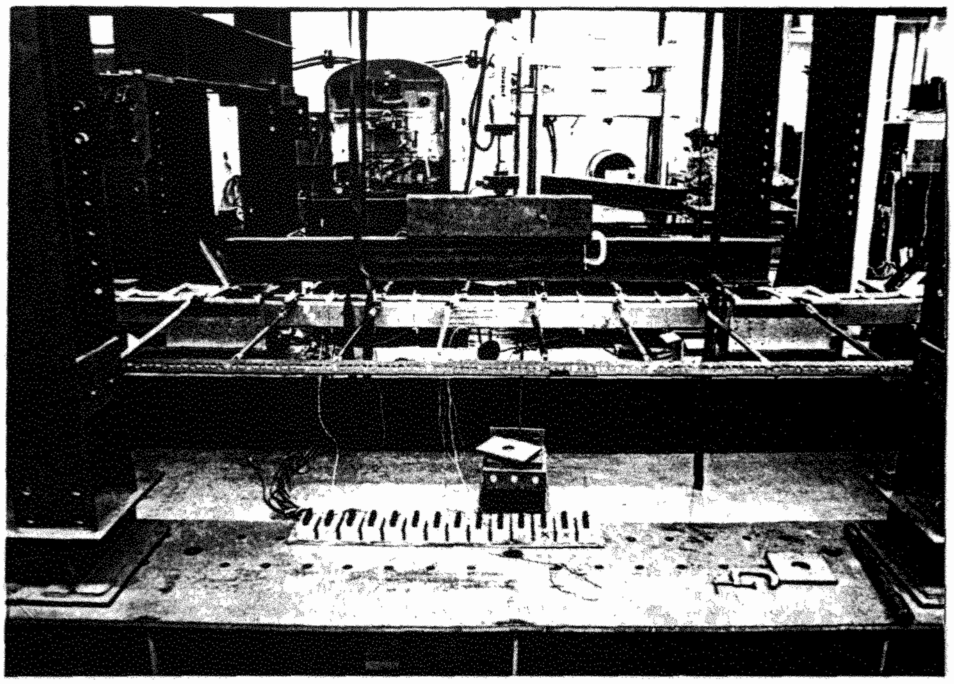

(a) side view

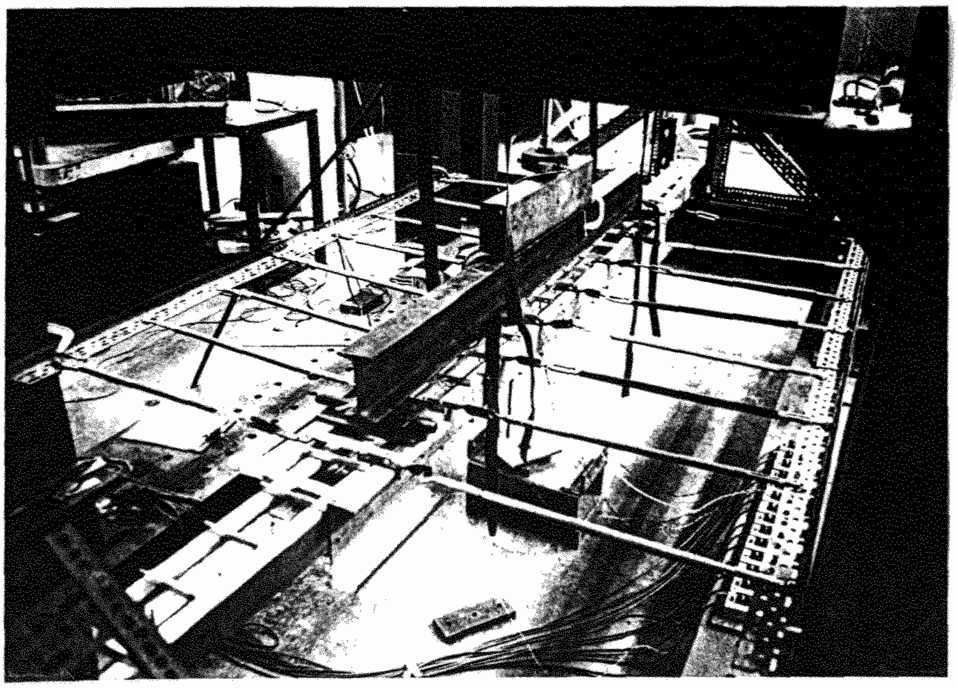

(b) top view

Figure 5. Typical Bracing System

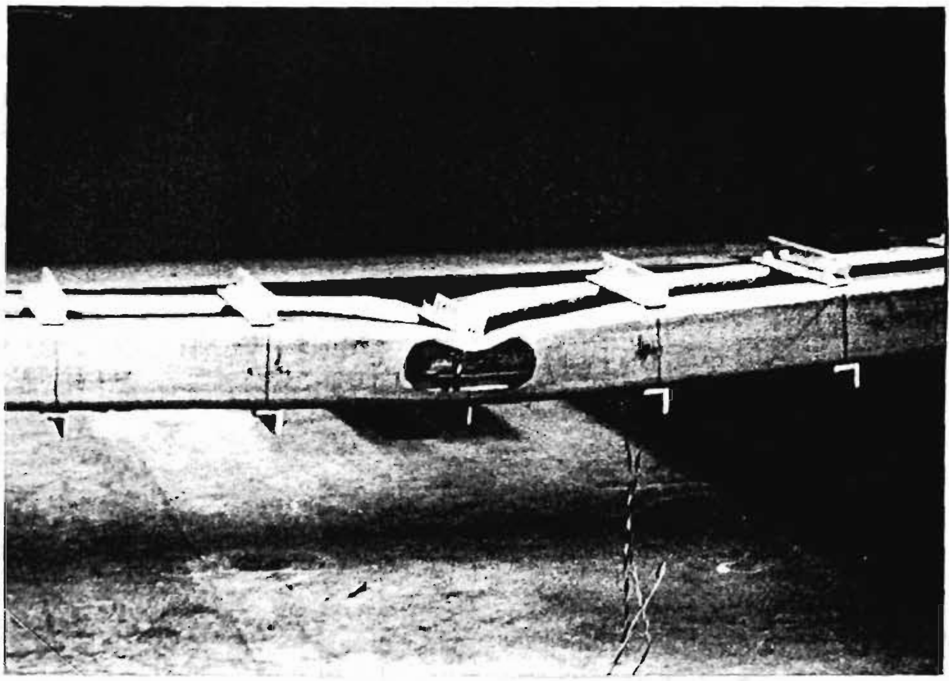

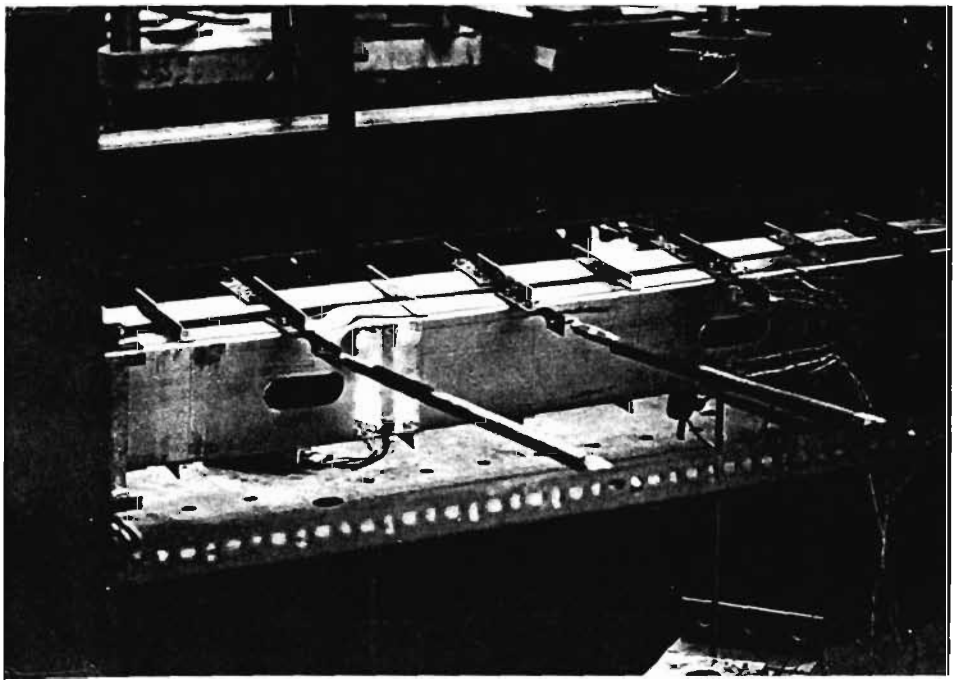

Figure 6. Typical Failure Pattern

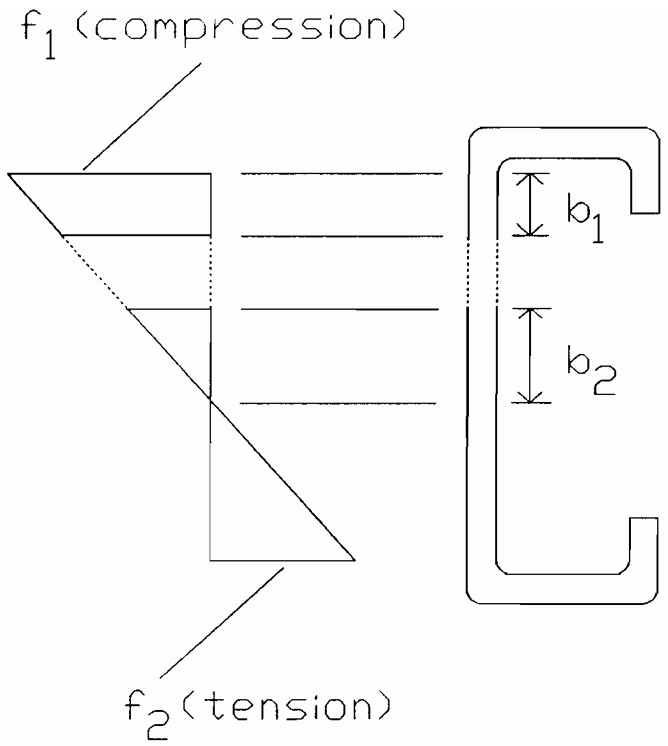

Figure 7. AISI for the Effective Web Area

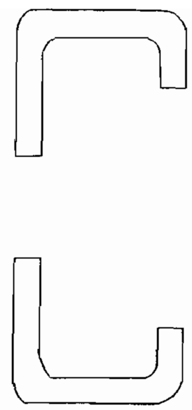

Figure 8. Net Section for Net Web Area

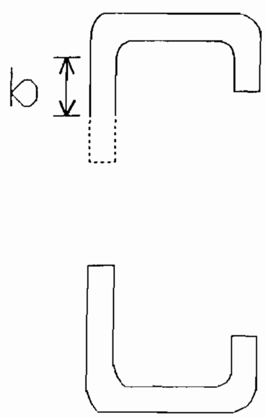

Figure 9. Net Section Using Unstiffened Compression Web Element

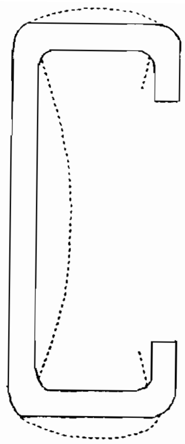

(a) local buckling mode

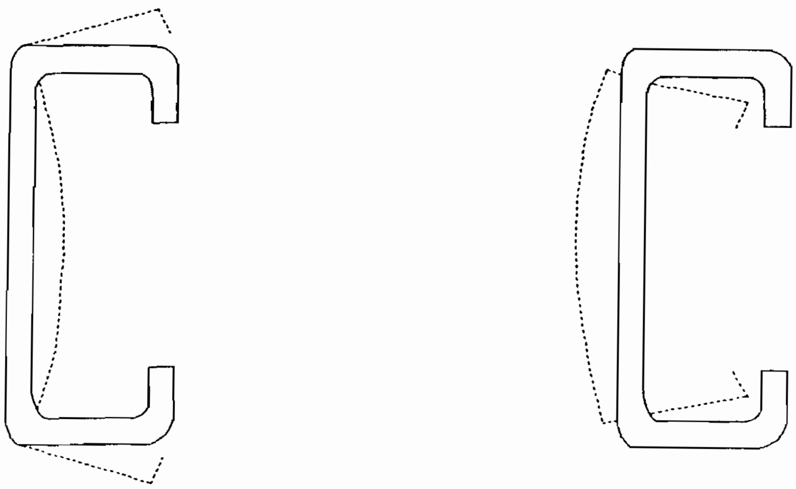

(b) distortional buckling modes

Figure 10. Local and Distortional Buckling Modes

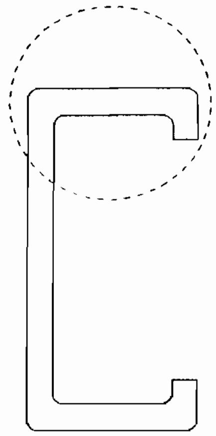

(a) real section

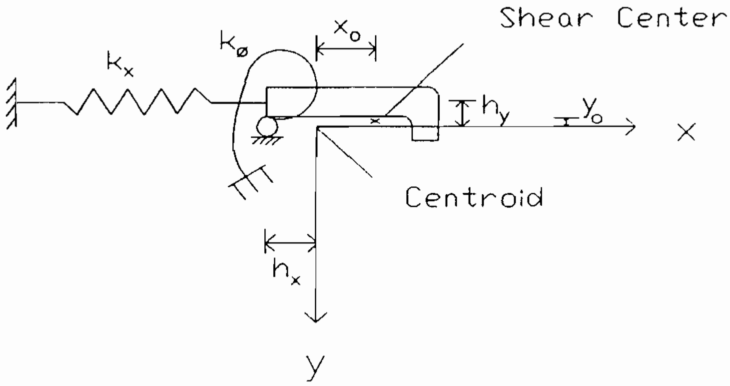

(b) model A

Figure 11. Analytical Model A for Distortional Buckling

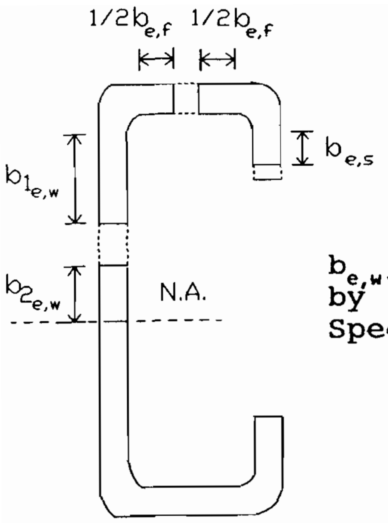

$b_{e,w}$, $b_{e,f}$ and $b_{e,s}$ are determined by $f=F_y$ and the equations of AISI Specification.

Figure 12a. Method I: $M_{uc,d} = F_d\ S_{ex,fy}$ for Effective Section Modulus

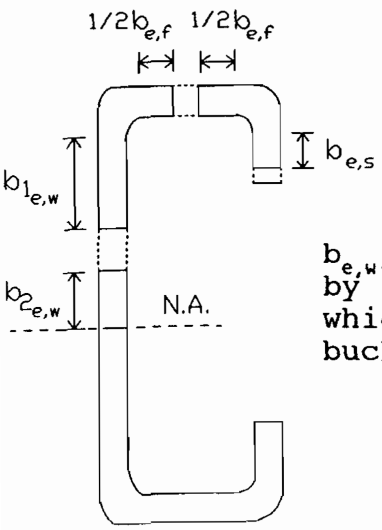

$b_{e,w}$, $b_{e,f}$ and $b_{e,s}$ are determined by $f=F_d$ and Eqs. 10a, 10b and 10c which account for the distortional buckling behaviour.

Figure 12b. Method II: $M_{uc,d} = F_d\ S_{ex,d}$ for Effective Section Modulus

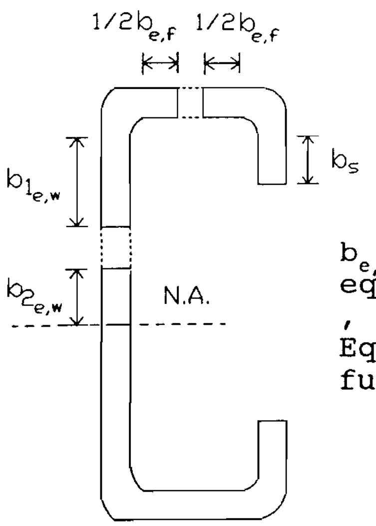

$b_{e,w}$ is determined by $f=F_d$ and the equations of AISI Specification, $b_{e,f}$ is determined by $f=F_d$ and Eqs. 10a, 10b and 10c and b_s is fully effective.

Figure 12c. Method III: $M_{uc,d}= F_d\ S_{ex,Fd}$ for Effective Section Modulus

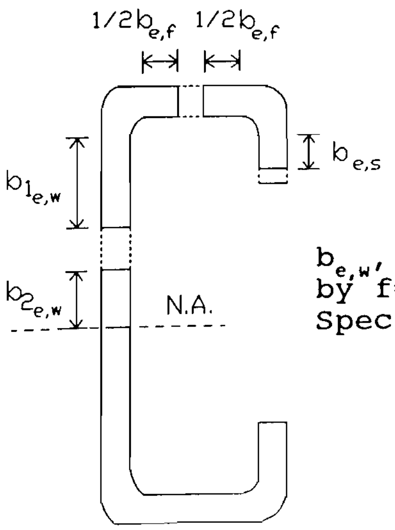

$b_{e,w}$, $b_{e,f}$ and $b_{e,s}$ are determined by $f=F_d$ and the equations of AISI Specification.

Figure 12d. Method IV: $M_{uc,d}= F_d\ S_{ex,dy}$ for Effective Section Modulus

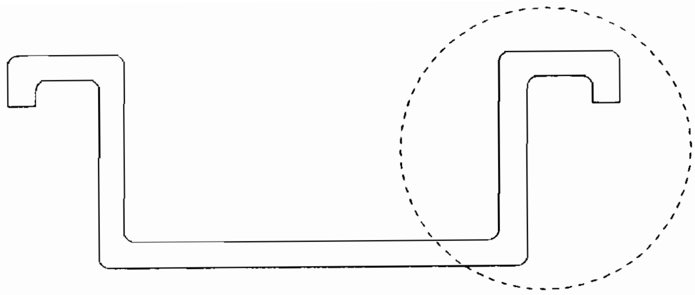

(a) real section

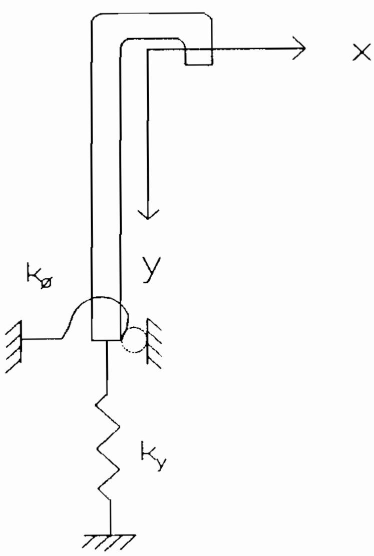

(b) model B

Figure 13. Analytical Model B for Distortional Buckling

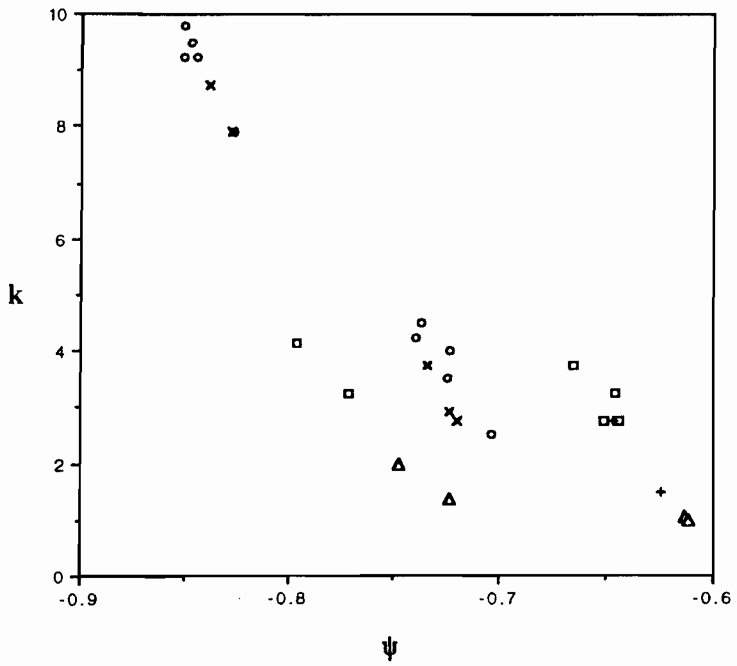

Figure 14a. Relationship between Buckling Coefficient k and ψ

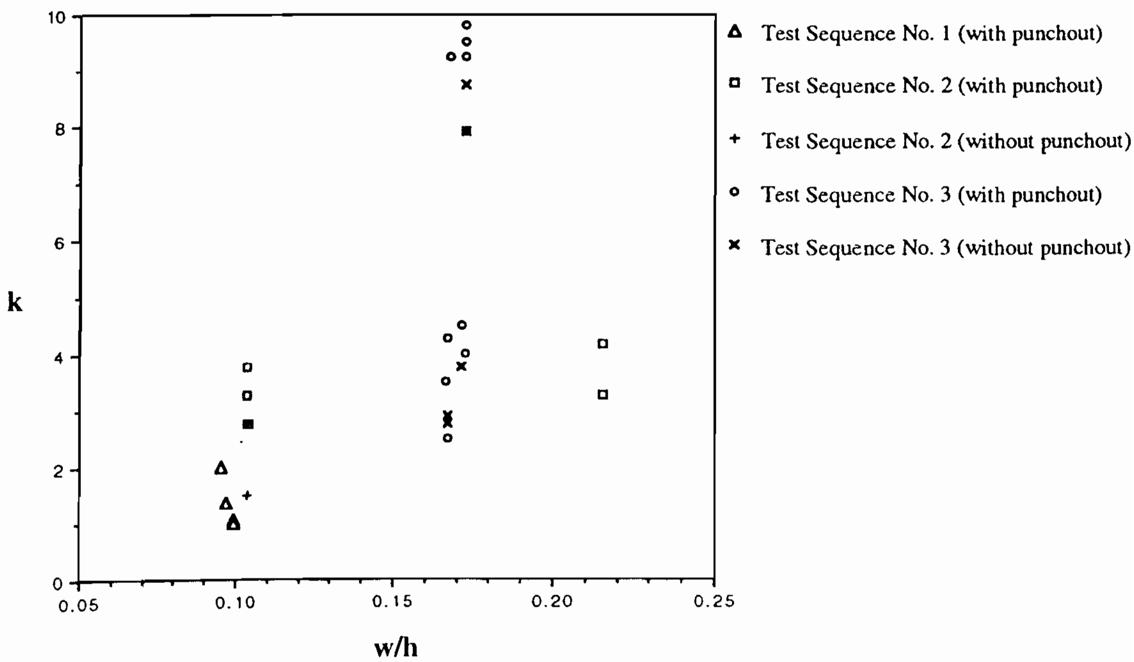

Figure 14b. Relationship between Buckling Coefficient k and w/h

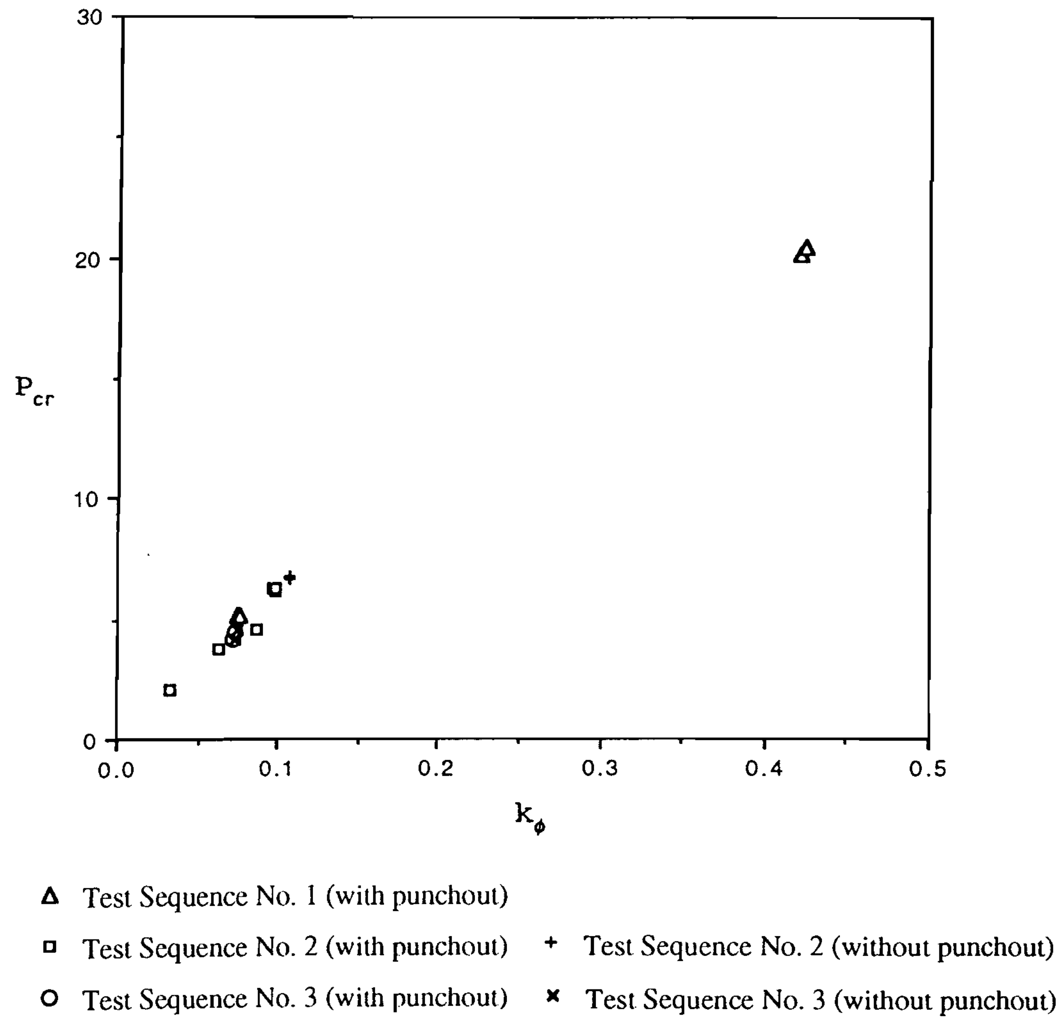

Figure 15. Relationship between the Buckling Load P_{cr} and Stiffness of Rotational Restraint k_ϕ

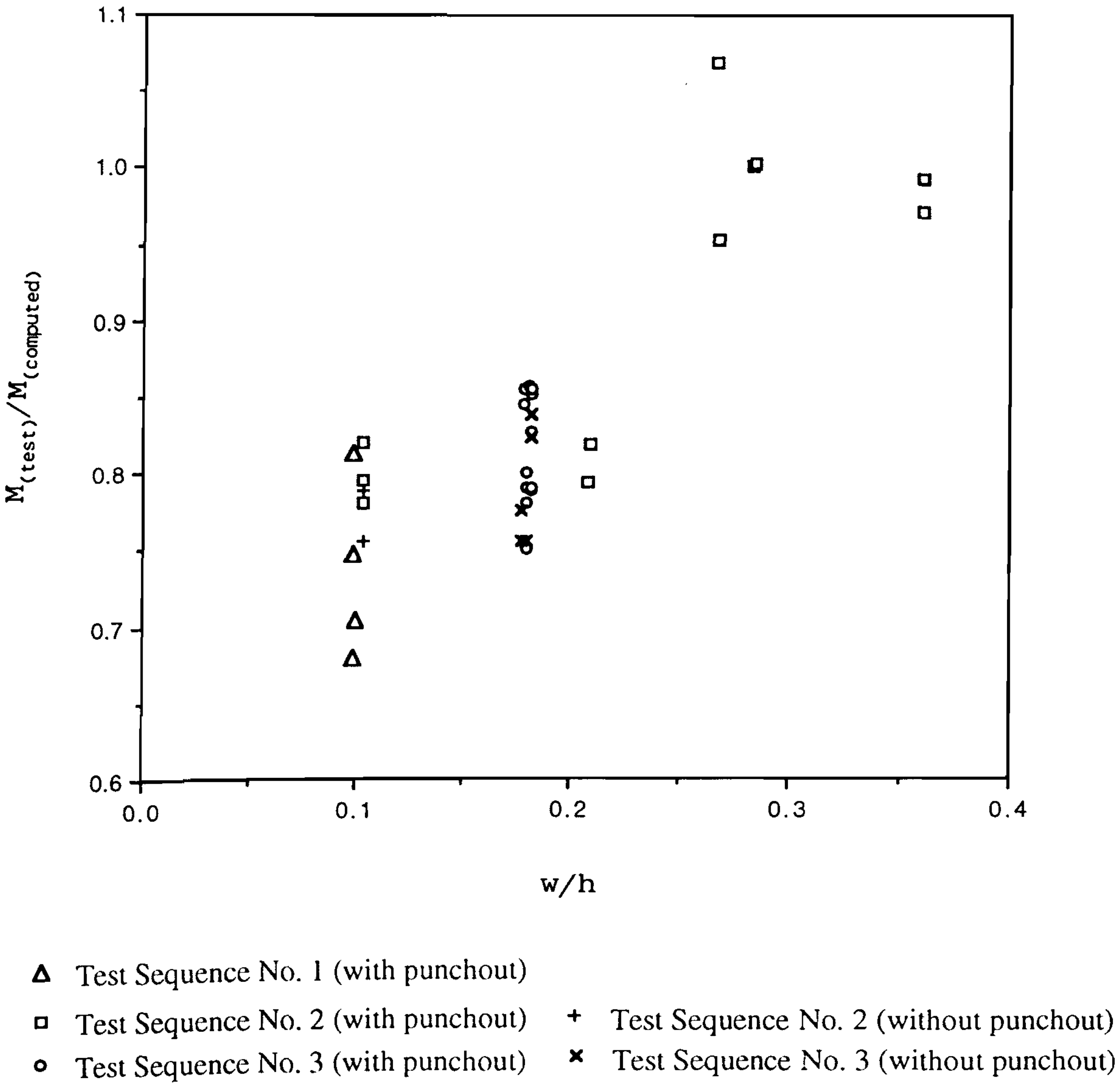

Figure 16. Relationship between the $M_{(test)}/M_{(computed)}$ and w/h